

Reactions of Sulfoxides with Reactive Oxygen Species to Reveal the Radical Chemistry of Pollution-Derived Particulate Matter

Carl P. Soltau,^a Zac E. Brown,^b Aidan J. Brock,^a Alexander P. Martyn,^c James P. Blinco,^a Branka Miljevic,^b John C. McMurtrie^a and Steven E. Bottle*^a

- ^a. School of Chemistry and Physics and Centre for Materials Science, Queensland University of Technology, Brisbane, QLD, 4000, Australia. E-mail: s.bottle@qut.edu.au
- ^b. School of Earth & Atmospheric Sciences, Queensland University of Technology, Brisbane, QLD, 4000, Australia.
- ^c. Cancer & Ageing Research Program, Centre for Genomics and Personalised Health at the Translational Research Institute (TRI), Woolloongabba, QLD,4102, Australia.

Supporting Information

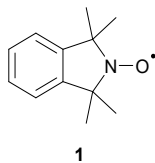
Table of Contents

General Experimental.....	2
Synthesis of 1,1,3,3-tetramethylisoindolin-2-yloxy (TMIO) (1)	2
Synthesis of Iminium Ion (9).....	3
General Procedure for Fe(II) and Cu(I)-Catalyzed Fenton Reactions.....	4
Characterisation Data of Isolated Compounds 2-7, 9-11	8
NMR Spectra.....	11
LC-MS Data	22
Single Crystal XRD of Compounds 4, 5, 7 & 9	32
Characterisation Data for Non-Isolated Products (12-15).....	36
D6-DMSO Experiment	39
Reactions with Iminium Ion (9).....	40
Pollution Derived-PM Experiments	42
References.....	50

General Experimental

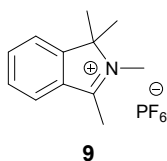
Phthalic anhydride ($\geq 99\%$), benzylamine ($\geq 99\%$), *m*CPBA (77%), iodine (99.8%), Pd/C (10 wt. %), iron(II) sulfate heptahydrate ($\geq 99\%$), copper(II) chloride (99%), iron(III) sulfate hydrate (97%), iron(III) chloride anhydrous (99.99%), hydrogen peroxide (30 wt. % in H₂O), Luperox TBH70X *tert*-butyl hydroperoxide (70 wt. % in H₂O) and hexafluorophosphoric acid (~55 wt. %) were purchased from Sigma Aldrich and used as received. Dimethyl sulfoxide (95%), tetrahydrothiophene-1-oxide (95%) and iodomethane (99%, stabilized with copper foil) was purchased from ChemSupply and used as received. Solvents glacial acetic acid (95% w/v) and dichloromethane (99.8 %) were purchased from Fischer Scientific and used as received. Diethyl ether anhydrous (99%) and toluene (99.5%) used in the synthesis of the Grignard reagent were purchased from Fischer Scientific and stored over sodium wire. Copper(I) chloride (97%) was purchased from Sigma Aldrich and purified by dissolving in 32% HCl and precipitation by water. The resulting solid was filtered and washed with ethanol and diethyl ether.^{1, 2} ¹H and ¹³C NMR were performed using a Bruker AVANCE III 600 MHz NMR Spectrometer at 25°C. Chemical shifts are reported as δ (ppm) relative to the solvent used. Abbreviations used include s = singlet, d = doublet, t = triplet, dd = doublet of doublets, dt = doublet of triplets, td = triplet of doublets, ddd = doublet of doublets of doublets, bd = broad doublet and m = multiplet. Analytical TLC was performed using Grace Reveleris Al-backed TLC Plates (UV254). Flash chromatography was performed using an Agilent Varian 971-FP Flash Chromatography Purification System w/ Column Station with a PuriFlash PF-30SIHP/25g column. Fourier-Transform Infrared (FT-IR) spectra were obtained using a Bruker ALPHA-P FT-IR spectrometer with ATR accessory. High-resolution Mass Spectra (HRMS) were obtained on a Thermo Scientific LTQ Orbitrap XL ETD Hybrid Ion Trap-Orbitrap Mass Spectrometer equipped with a heated electrospray ionization (ESI) source operating in positive ion mode at a mass resolution of 120,000 (at *m/z* 400). Analytical reversed-phase HPLC (RP-HPLC) was performed using a Thermo Scientific Dionex UltiMate 3000 RSLC and an Agilent Prep-C18 Scalar column (10 μ , 150 \times 4.6 mm) at 0.8 mL min⁻¹. For analytical RP-HPLC, compounds were eluted using an isocratic method with 0.1% formic acid (FA) in H₂O (solvent A) and 100% MeOH (solvent B) in at 40°C. Unless otherwise stated, elution conditions were; Solvent A: 0.1% FA in H₂O, Solvent B: MeOH. Isocratic (0.8 mL/min): 20% A with 80% B at 40°C detecting at 254 nm.

Synthesis of 1,1,3,3-tetramethylisoindolin-2-yloxy (TMIO) (1)



Synthesis of **1** was achieved over a 4-step process using literature established procedures,^{3, 4} starting from commercially available maleic anhydride. Maleic anhydride was reacted with benzylamine in high yield (95%) before being added to excess Grignard reagent (MeMgI) to give 36% of 2-benzyl-1,1,3,3-tetramethylisoindoline.⁴ The benzyl group was cleaved by hydrogenation to give 1,1,3,3-tetramethylisoindoline in high yield (97%).⁴ This secondary amine was then treated with *m*CPBA (1.5 eqv.) to afford **1** as a crystalline yellow solid (99%).³ IR (neat) 3046 w, 2974 m, 2927 m, 2863 w, 1451 m, 760 s; HRMS (ESI) *m/z* calcd for C₁₂H₁₇NO[•]: 190.1232 [*M*]⁺; found: 190.1229; *m/z* calcd for C₁₁H₁₄NO⁺: 176.1070 [*M*-CH₃+H]⁺; found: 176.1073. Mp: 123-124°C (lit.⁵ 123-125). HPLC: *t_R* = 3.54 min, purity: >95%.

Synthesis of Iminium Ion (9)



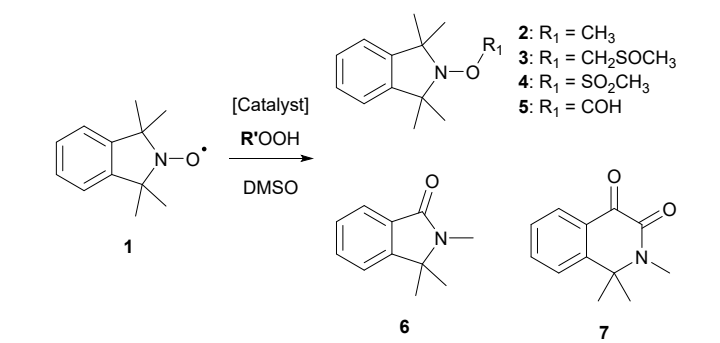
Nitroxide **1** (100 mg, 0.53 mmol) was dissolved in DMSO (3 mL) with stirring. To this solution, Fe₂(SO₄)₃ (525 mg, 1.31 mmol). The reaction was stirred at room temperature until consumption of starting material by TLC. Upon completion, deionised water (100 mL) was added and the aqueous phase was extracted with diethyl ether (1 x 50 mL). The aqueous layer was adjusted to pH 14 with 5 M NaOH and extracted with diethyl ether (2 x 50 mL). The organic layer was separated and dried over anhydrous Na₂SO₄ before it was decanted into a separate dry flask. To this flask an excess of HPF₆ ~55 wt. % (1 mL) was added and stirred, resulting in the formation of a precipitate. The precipitate was collected by vacuum filtration and washed with deionised water (1 x 10 mL) and diethyl ether (1 x 10 mL) to afford **9** as a white solid (151 mg, 90%).
¹H NMR (600 MHz, CD₃CN): δ=8.07 (d, *J*=7.8 Hz, 1H, Ar-H), 7.91 (td, *J*=7.6, 0.9 Hz, 1H, Ar-H), 7.76 (d, *J*=7.7 Hz, 1H, Ar-H), 7.71 (td, *J*=7.7, 0.8 Hz, 1H, Ar-H), 3.58 (s, 3H, CH₃), 2.79 (s, 3H, CH₃), 1.63 (s, 6H, CH₃); ¹³C NMR (150 MHz, CD₃CN): δ=179.5 (C=N⁺), 154.1 (Ar-C), 136.8 (Ar-C), 132.7 (Ar-C), 130.8 (Ar-C), 127.1 (Ar-C), 122.9 (Ar-C), 78.5 (q-C), 32.5 (CH₃), 23.0 (CH₃), 14.8 (CH₃); ¹⁹F NMR (564 MHz, CD₃CN): δ= -72.92 (bd, *J*_{F-P}=706.9 Hz); IR (neat); 2991 m, 2943 m, 1627 w, 1583 w, 826 s, 771 s, 556 s; HRMS (ESI) *m/z* calcd for C₁₂H₁₆N⁺: 174.1277 [*M*]⁺; found: 174.1281; Mp: 170–171 °C. HPLC: *t*_R = 1.34 min, purity: 99%.

The above procedure was also carried out at the same scale with CuCl₂·2H₂O (223 mg, 1.31 mmol) replacing Fe₂(SO₄)₃ which provided 133 mg (85%) of iminium ion **9**.

General Procedure for Fe(II) and Cu(I)-Catalyzed Fenton Reactions

TMIO **1** (1.05 mmol, 1.0 eqv.) was dissolved in DMSO (3 mL) with stirring. To this FeSO₄·7H₂O (2.60 mmol, 2.5 eqv.) or CuCl (0.10 mmol, 0.1 eqv) was added followed by dropwise addition of H₂O₂/TBHP (5.2 mmol, 5.0 eqv.) over 1hr *via* syringe pump. The reaction was stirred at room temperature and monitored by TLC for consumption of starting material for up to 24 h. Upon completion the reaction was diluted with deionised water (100 mL) and extracted with diethyl ether (3 x 50 mL). The organic layer was separated and dried over anhydrous Na₂SO₄ and concentrated *in vacuo*. The crude material was purified by flash chromatography to afford **2-7** & **10-13** in their corresponding yields.

Table 1. Reaction conditions and isolated yields for the Fe(II)/Cu(I)-catalysed reactions of hydrogen peroxide and *tert*-butyl hydroperoxide (TBHP) with DMSO in the presence of nitroxide **1**.



2: R₁ = CH₃
 3: R₁ = CH₂SOCH₃
 4: R₁ = SO₂CH₃
 5: R₁ = COH

Entry	Catalyst	R'	Time ^[a] (h)	Yield ^[b] (%)						
				2	3	4	5	6	7	
1	Fe ²⁺	H	1.5	85	-	5	-	-	-	
2	Cu ⁺	H	2.0	45	-	45	-	-	-	
3	Fe ²⁺	<i>t</i> Bu	1.5	60	27	-	-	-	-	
4	Cu ⁺	<i>t</i> Bu	22.0	20	18	7	6	12	7	

[a] Time at which starting material nitroxide **1** was fully consumed by TLC. [b] Isolated yield after flash chromatography.

Table 1, Entry 1

The general procedure was followed in DMSO with **1** (200 mg, 1.05 mmol), FeSO₄·7H₂O (731 mg, 2.63 mmol) and H₂O₂ (527 μL, 5.26 mmol). Starting material was consumed after 1.5 h. Flash chromatography (hexane:ethyl acetate) afforded 183 mg (85%) of **2** and 5.6 mg (5%) of **4**.

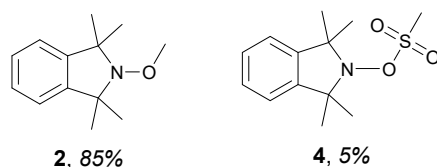


Table 1, Entry 2

The general procedure was followed in DMSO with **1** (197 mg, 1.03 mmol), CuCl (10.4 mg, 0.10 mmol) and H₂O₂ (519 μL, 5.18 mmol). Starting material was consumed after 2 hrs. Flash chromatography (hexane:ethyl acetate) afforded 95 mg (45%) of **2** and 125 mg (45%) of **4**.

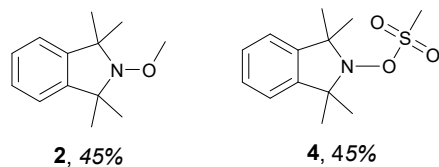


Table 1, Entry 3

The general procedure was followed in DMSO with **1** (200 mg, 1.05 mmol), FeSO₄·7H₂O (731 mg, 2.63 mmol) and TBHP (720 μL, 5.26 mmol). Starting material was consumed after 1.5 h. Flash chromatography (hexane:ethyl acetate) afforded 129 mg (60%) of **2** and 76 mg (27%) of **3**.

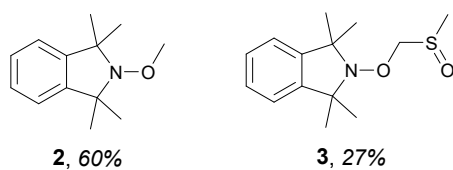


Table 1, Entry 4

The general procedure was followed in DMSO with **1** (203 mg, 1.07 mmol), CuCl (10.7 mg, 0.11 mmol) and TBHP (730 μL, 5.33 mmol). Starting material was consumed after 22 hrs. Flash chromatography (hexane:ethyl acetate) afforded 43 mg (20%) of **2**, 51 mg (18%) of **3**, 20 mg (7%) of **4**, 18 mg (6%) of **5**, 22 mg (12%) of **6** and 15 mg (7%) of **7**.

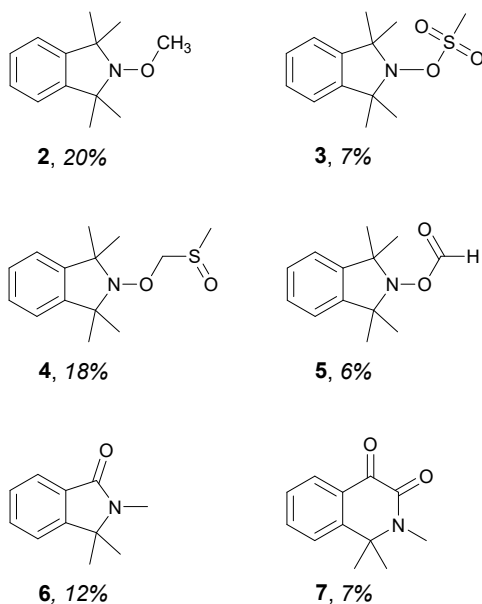
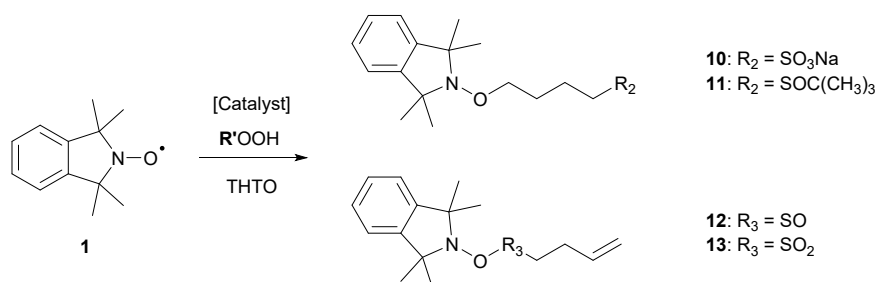


Table 2. Reaction conditions and isolated yields for the Fe(II)/Cu(I)-catalysed reactions of hydrogen peroxide and *tert*-butyl hydroperoxide with THTO in the presence of nitroxide **1**.



Entry	Catalyst	R' =	Time ^[a] (h)	Yield ^[b] (%)			
				10	11	12	13
1	Fe ²⁺	H	1.5	85	-	-	-
2	Cu ⁺	H	2.0	-	-	-	-
3	Fe ²⁺	<i>t</i> Bu	1.5	-	85	5	5
4	Cu ⁺	<i>t</i> Bu	22.0	-	83	5	5

[a] Time at which starting material nitroxide **1** was fully consumed by TLC. [b] Isolated yield after flash chromatography.

Table 2, Entry 1

The general procedure was followed in THTO with **1** (222 mg, 1.12 mmol), FeSO₄·7H₂O (800 mg, 2.91 mmol) and H₂O₂ (585 μL, 5.84 mmol). Starting material was consumed after 1.5 hrs. The aqueous phase was made slightly basic (pH ~8) with NaOH and gravity filtered through a fritted glass funnel. The filtrate was then made slightly acidic (pH 6.5 – 6.9) with HCl before being frozen with liquid N₂ and the solvent removed by freeze-drying. The remaining crude material was then purified by reversed-phase flash chromatography (H₂O:MeOH) to afford 346 mg (85%) of **10**.

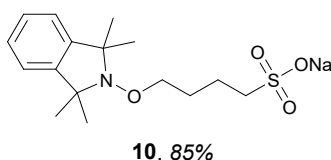


Table 2, Entry 2

The general procedure was followed in THTO with **1** (200 mg, 1.05 mmol), FeSO₄·7H₂O (731 mg, 2.63 mmol) and H₂O₂ (527 μL, 5.26 mmol). Reaction was monitored by TLC periodically over a total of 24 hours which revealed the presence of starting material. Upon workup ~95% starting material recovered.

*Notes: Despite optimisation attempts this reaction could not be improved to allow the full consumption of nitroxide **1** with only trace amounts of THTO-derived products **13** and **14** detected by RP-HPLC over a 24-hour period. Variations of the addition time of hydrogen peroxide saw effervescence increase with a shorter addition time (0.1 h) and decrease over a longer addition period (5 h), however neither approach showed any significant increase of nitroxide **1** consumption by RP-HPLC. The hydrogen peroxide was also diluted from 30% (w/w) to 10% (w/w) and 5% (w/w) and added over a 1 or 5 hour period which lowered the intensity of the effervescence but again no improvement on nitroxide **1** consumption was observed.*

Table 2, Entry 3

The general procedure was followed in THTO with **1** (195 mg, 1.03 mmol), Fe₂SO₄·7H₂O (712 mg, 2.56 mmol) and TBHP (702 μL, 5.13 mmol). Starting material was consumed after 1.5 hrs. Flash chromatography

(hexane:ethyl acetate) afforded 320 mg (85%) of **11** and 20 mg of **12** (5%) and **13** (5%) as a mixture (ratio determined by NMR).

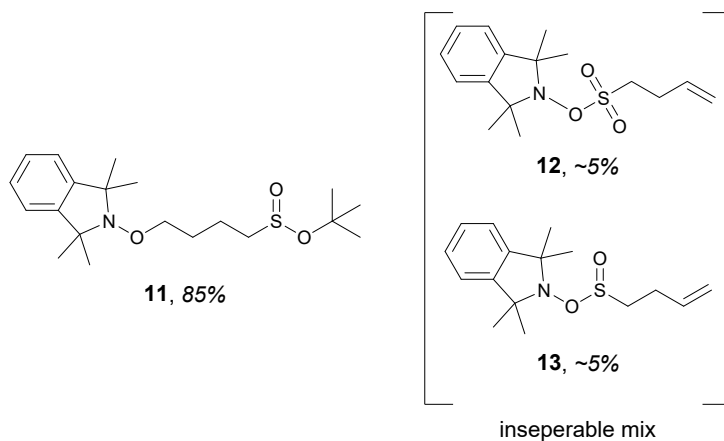
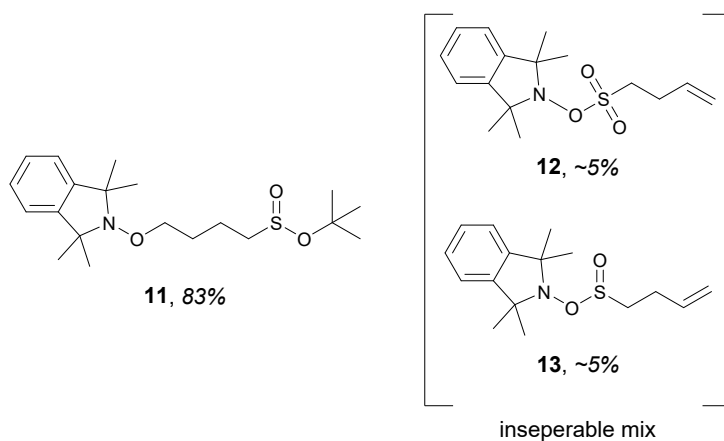


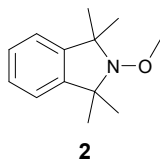
Table 2, Entry 4

The general procedure was followed in THFO with **1** (201 mg, 1.06 mmol), CuCl (10.6 mg, 0.11 mmol) and TBHP (723 μ L, 5.28 mmol). Starting material was consumed after 1.5 hrs. Flash chromatography (hexane:ethyl acetate) afforded 322 mg (83%) of **11** and 20 mg of **12** (5%) and **13** (5%) as a mixture (ratio determined by NMR).



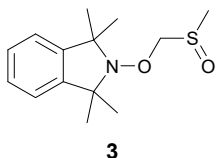
Characterisation Data of Isolated Compounds 2-7, 9-11

2-Methoxy-1,1,3,3-tetramethylisoindoline (2)



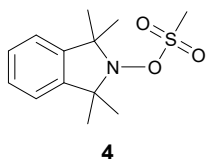
Low melting white crystalline solid. ^1H NMR (600 MHz, CDCl_3): δ =7.30–7.16 (m, 4H; Ar-H), 3.86 (s, 3H; CH_3), 1.51 (s, 12H; CH_3); ^{13}C NMR (150 MHz, CDCl_3): δ =145.3 (Ar-C), 127.3 (Ar-C), 121.6 (Ar-C), 67.2 (q-C), 65.6 (N-O- CH_3), 30.1 (CH_3), 25.3 (CH_3); IR (neat); 3073 m, 2977 m, 2891 m, 1457 m, 1357 m, 1268 m, 1166 m, 1049 s, 753 s; HRMS (ESI) m/z calcd for $\text{C}_{13}\text{H}_{20}\text{NO}^+$: 206.1539 [$M+\text{H}$] $^+$; found: 206.1540. M.p. = 38–39°C. HPLC: t_R = 11.13 min, purity: 99%.

1,1,3,3-Tetramethyl-2-((methylsulfinyl)methoxy)isoindoline (3)



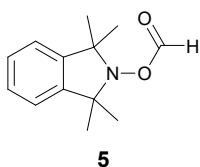
White crystalline solid. ^1H NMR (600 MHz, CDCl_3): δ =7.27–7.10 (m, 4H, Ar-H), 4.98 (d, J =10.3 Hz, 1H, CH_2), 4.81 (d, J =10.3 Hz, 1H, CH_2), 2.64 (s, 3H, CH_3), 1.60–1.37 (m, 12H, CH_3); ^{13}C NMR (150 MHz, CDCl_3): δ =143.9 (Ar-C), 127.9 (Ar-C), 121.7 (Ar-C), 94.2 (CH_2), 68.8 (q-C), 36.1 (CH_3), 30.0 (CH_3), 25.5 (CH_3); IR (neat); 2965 m, 2926 m, 2902 m, 1081 s, 1047 s, 961 m, 751 s; HRMS (ESI) m/z calcd for $\text{C}_{14}\text{H}_{22}\text{NO}_2\text{S}^+$: 268.1366 [$M+\text{H}$] $^+$; found: 268.1368; m/z calcd for $\text{C}_{14}\text{H}_{21}\text{NO}_2\text{SNa}^+$: 290.1185 [$M+\text{Na}$] $^+$; found: 290.1188; m/z calcd for $\text{C}_{28}\text{H}_{42}\text{N}_2\text{O}_4\text{S}_2\text{Na}^+$: 557.2478 [$2M+\text{Na}$] $^+$; found: 557.2484. M.p. = 79–80°C. HPLC: t_R = 3.78 min, purity: 95%.

1,1,3,3-Tetramethylisoindolin-2-yl methanesulfonate (4)



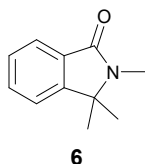
White crystalline solid. ^1H NMR (600 MHz, CDCl_3): δ =7.30–7.11 (m, 4H, Ar-H), 3.18 (s, 3H, CH_3), 1.64 (s, 6H, CH_3), 1.48 (s, 6H, CH_3); ^{13}C NMR (150 MHz, CDCl_3): δ =143.2 (Ar-C), 128.2 (Ar-C), 121.8 (Ar-C), 70.8 (q-C), 36.4 ($\text{SO}_3\text{-CH}_3$), 30.2 (CH_3), 26.1 (CH_3); IR (neat); 3005 m, 2980 m, 2929 m, 1338 s, 1179 s, 917 s, 810 s, 776 s; HRMS (ESI) m/z calcd for $\text{C}_{13}\text{H}_{20}\text{NO}_3\text{S}^+$: 270.1158 [$M+\text{H}$] $^+$; found: 270.1162. M.p. = 130–131°C (decomp). HPLC: t_R = 3.84 min, purity: 99%.

1,1,3,3-Tetramethylisoindolin-2-yl formate (5)



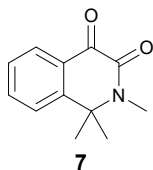
White crystalline solid. ^1H NMR (600 MHz, CDCl_3): δ =8.49 (s, 1H, CHO), 7.31–7.14 (m, 4H, Ar-H), 1.47–1.43 (overlapped, 12H, CH_3); ^{13}C NMR (150 MHz, CDCl_3): δ = 167.9 (RCHO), 143.4 (Ar-C), 128.1 (Ar-C), 121.8 (Ar-C), 68.2 (q-C), 28.6 (CH_3), 25.5 (CH_3); IR (neat); 3469 vw, 2982 m, 2958 m, 2923 m, 2868 w, 1740 s, 1456 m, 1366 m, 1265 m, 1134 s, 1103 s, 767 s, 654 s; HRMS (ESI) m/z calcd for $\text{C}_{13}\text{H}_{18}\text{NO}_2^+$: 220.1332 [$M+\text{H}$] $^+$; found: 220.1340. M.p. = 102–103°C (decomp). HPLC: t_R = 5.04 min, purity: 99%.

2,3,3-Trimethylisoindolin-1-one (6)



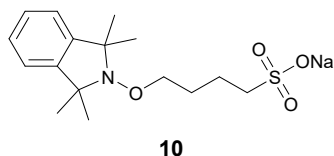
Viscous lightly-coloured oil. ^1H NMR (600 MHz, CDCl_3): δ =7.82 (dt, J =7.5, 0.8 Hz, 1H, Ar-H), 7.53 (td, J =7.4, 1.1 Hz, 1H, Ar-H), 7.43–7.40 (overlapped, 2H, Ar-H), 3.03 (s, 3H, CH_3), 1.45 (s, 6H, CH_3); ^{13}C NMR (150 MHz, CDCl_3): δ =167.4 (C=O), 151.7 (Ar-C), 131.6 (Ar-C), 131.1 (Ar-C), 128.1 (Ar-C), 123.7 (Ar-C), 120.8 (Ar-C), 62.2 (q-C), 25.1 (CH_3), 24.0 (CH_3); HRMS (ESI) m/z calcd for $\text{C}_{11}\text{H}_{14}\text{NO}^+$: 176.1070 [$M+\text{H}$] $^+$; found: 176.1074. HPLC: t_R = 2.47 min, purity: 99%. Data agrees with literature.⁶

1,1,2-Trimethyl-1,2-dihydroisoquinoline-3,4-dione (7)



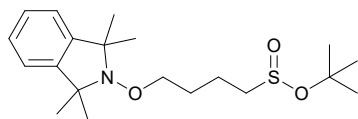
Lightly-coloured crystalline solid. ^1H NMR (600 MHz, CDCl_3): δ =8.21 (dd, J =7.9, 1.0 Hz, 1H, Ar-H), 7.71 (ddd, J =7.2, 1.5 Hz, 1H, Ar-H), 7.52 (d, J =8.1 Hz, 1H, Ar-H), 7.49 (ddd, J =7.3, 1.1 Hz, 1H, Ar-H), 3.26 (s, 3H, CH_3), 1.75 (s, 6H, CH_3); ^{13}C NMR (150 MHz, CDCl_3): δ =177.1 (C=O), 156.0 (C=O), 148.2 (Ar-C), 134.9 (Ar-C), 128.6 (Ar-C), 128.4 (Ar-C), 128.4 (Ar-C), 126.3 (Ar-C), 61.3 (q-C), 30.0 (CH_3), 29.7 (CH_3); IR (neat); 2976 m, 2929 m, 2865 w, 1693 m, 1653 s, 1641 s, 1601 m, 1278 s, 762 s; HRMS (ESI) m/z calcd for $\text{C}_{12}\text{H}_{14}\text{NO}_2^+$: 204.1019 [$M+\text{H}$] $^+$; found: 204.1021; m/z calcd for $\text{C}_{12}\text{H}_{13}\text{NO}_2\text{Na}^+$: 226.0838 [$M+\text{Na}$] $^+$; found: 226.0840; m/z calcd for $\text{C}_{24}\text{H}_{26}\text{N}_2\text{O}_4\text{Na}^+$: 429.1785 [$2M+\text{Na}$] $^+$; found: 429.1788. M.p. = 123–125°C (decomp). HPLC: t_R = 2.18 min, purity: 99%.

Sodium 4-((1,1,3,3-tetramethylisoindolin-2-yl)oxy)butane-1-sulfonate (10)



White solid. ^1H NMR (600 MHz, MeOD): δ =7.22–7.09 (m, 4H, Ar-H), 3.97 (t, J =6.3 Hz, 2H, CH_2), 2.88 (m, 2H, CH_2), 1.98 (m, 2H, CH_2), 1.78 (m, 2H, CH_2), 1.42 (s, 12H, CH_3); ^{13}C NMR (150 MHz, MeOD): δ =146.4 (Ar-C), 128.3 (Ar-C), 122.5 (Ar-C), 78.0 (CH_2), 68.4 (q-C), 52.7 (CH_2), 29.5 (CH_2), 23.5 (CH_2); IR (neat); 3532 w, 2971 w, 2928 w, 2870 w, 1723 w, 1454 w, 1187 s, 1048 s, 750 s, 609 s, 529 m; HRMS (ESI) m/z calcd for $\text{C}_{16}\text{H}_{25}\text{NO}_4\text{SNa}^+$: 350.1397 [$M+\text{H}$] $^+$; found: 350.1403. M.p. = 270–271 °C. HPLC: t_R = 7.36 min, purity: 96%.

Tert-butyl 4-((1,1,3,3-tetramethylisoindolin-2-yl)oxy)butane-1-sulfinate (11)



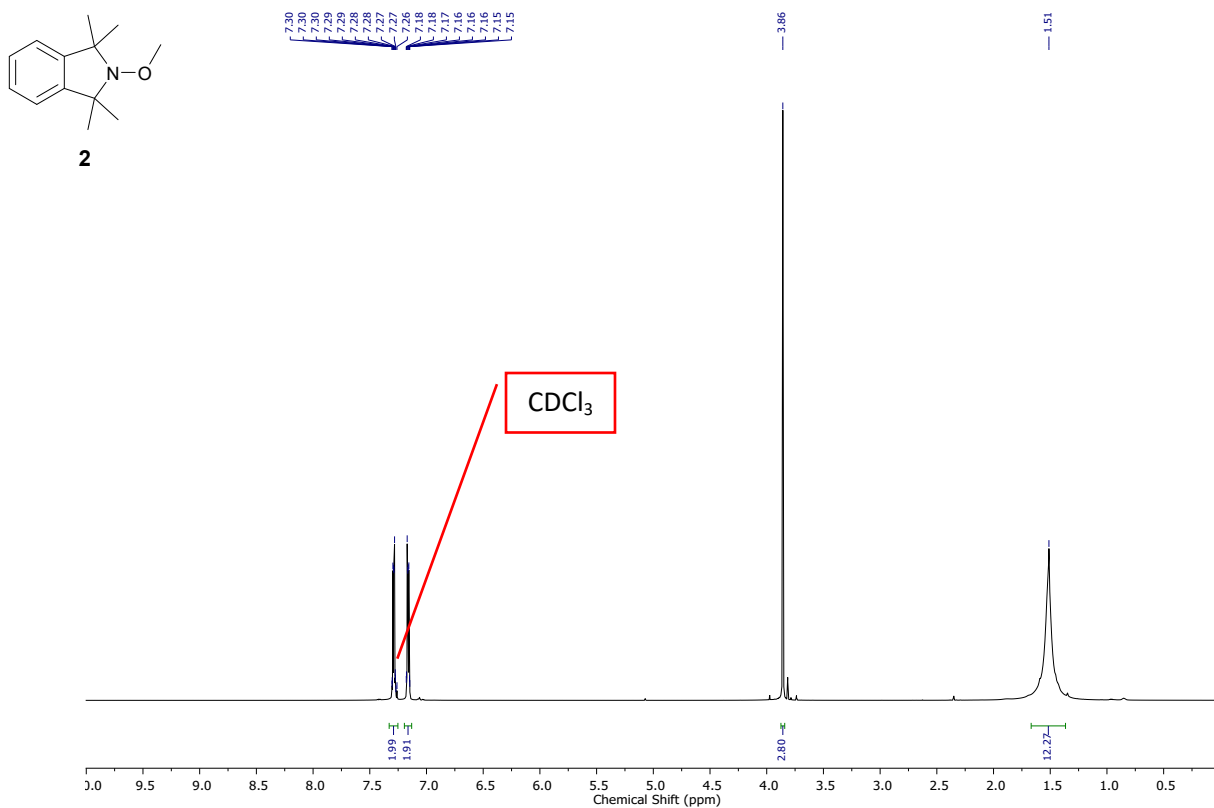
11

Low melting white solid. ^1H NMR (600 MHz, CDCl_3): δ =7.24-7.08 (m, 4H, Ar-H), 3.95 (t, J =6.1 Hz, 2H, CH_2) 2.77 (m, 2H, CH_2), 1.85 (m, 2H, CH_2), 1.77 (m, 2H, CH_2), 1.46-1.42 (overlapped, 21H, CH_3); ^{13}C NMR (150 MHz, CDCl_3): δ =145.3 (Ar-C), 127.3 (Ar-C), 121.6 (Ar-C), 82.0 (q-C), 76.7 (CH_2), 67.3 (q-C), 57.9 (CH_2), 29.9 (CH_3), 28.5 (CH_2) and 19.3 (CH_2); IR (neat); 2972 m, 2928 m, 2870 w, 1453 w, 1370 m, 1168 m, 1113 s, 1012 m, 859 s, 787 s, 770 s, 696 m, 658 m; HRMS (ESI) m/z calcd for $\text{C}_{20}\text{H}_{34}\text{NO}_3\text{S}^+$: 368.2254 [$M+\text{H}$] $^+$; found: 368.2263; m/z calcd for $\text{C}_{20}\text{H}_{33}\text{NO}_3\text{SNa}^+$: 390.2073 [$M+\text{Na}$] $^+$; found: 390.2080. M.p = 34-35 °C. HPLC: t_{R} = 13.39 min, purity 99%.

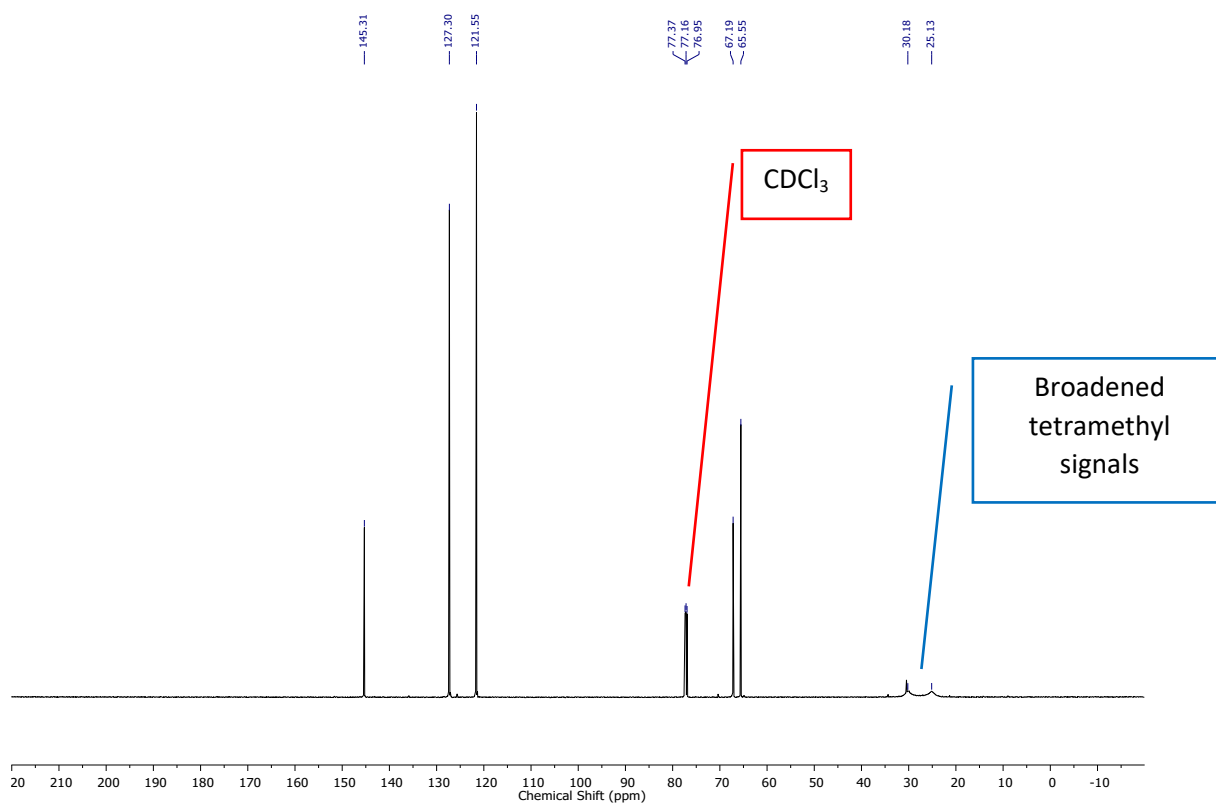
NMR Spectra

Note: ^1H and ^{13}C NMR signals of the tetramethyl groups of these molecules are often broadened by slow N-inversion and ring flipping on the NMR timescale. Consequently, they sometimes appear as two broadened lumps or as a single broad feature and sometimes as 3 or 4 broadened features. The sharpness and multiplicity of the signals is also dependant on the substituant on the the N-O bond.

2-Methoxy-1,1,3,3-tetramethylisoindoline (2)

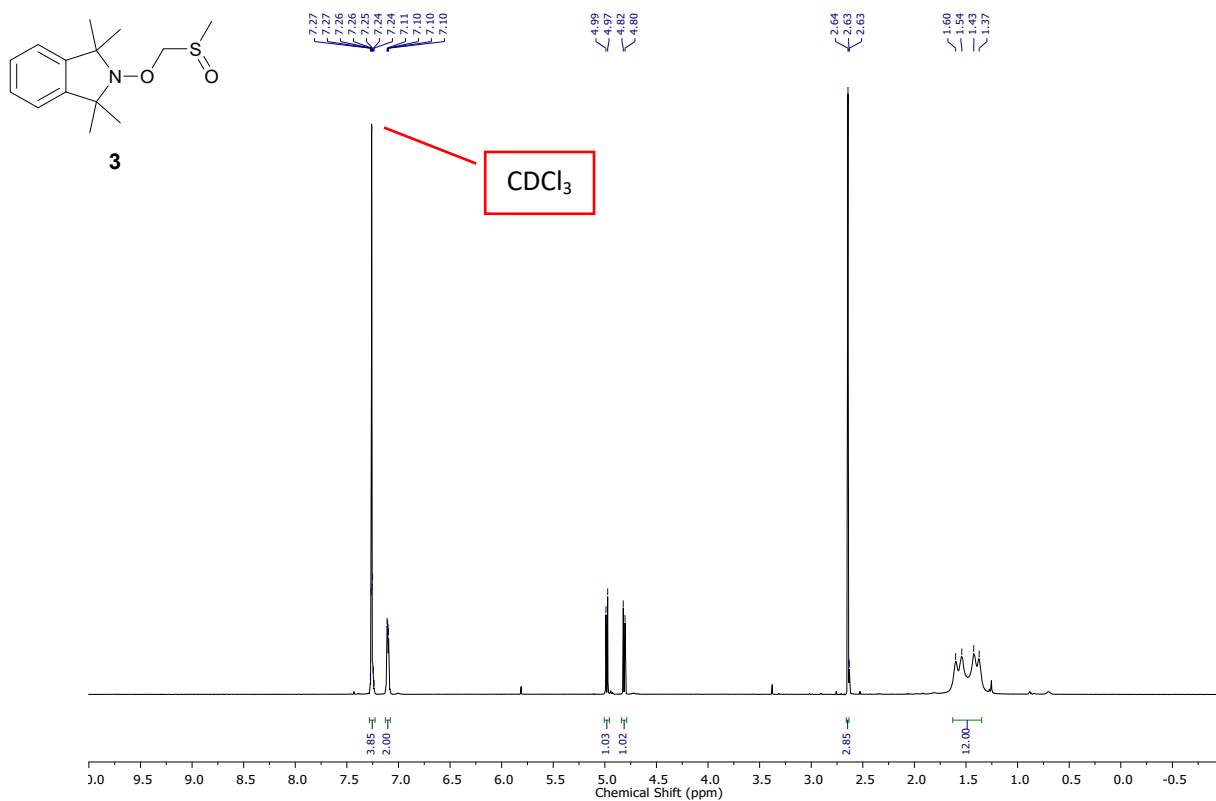


Supplementary Figure 1. ¹H NMR (600 MHz, CDCl₃) spectrum of 2-methoxy-1,1,3,3-tetramethylisoindoline 2.

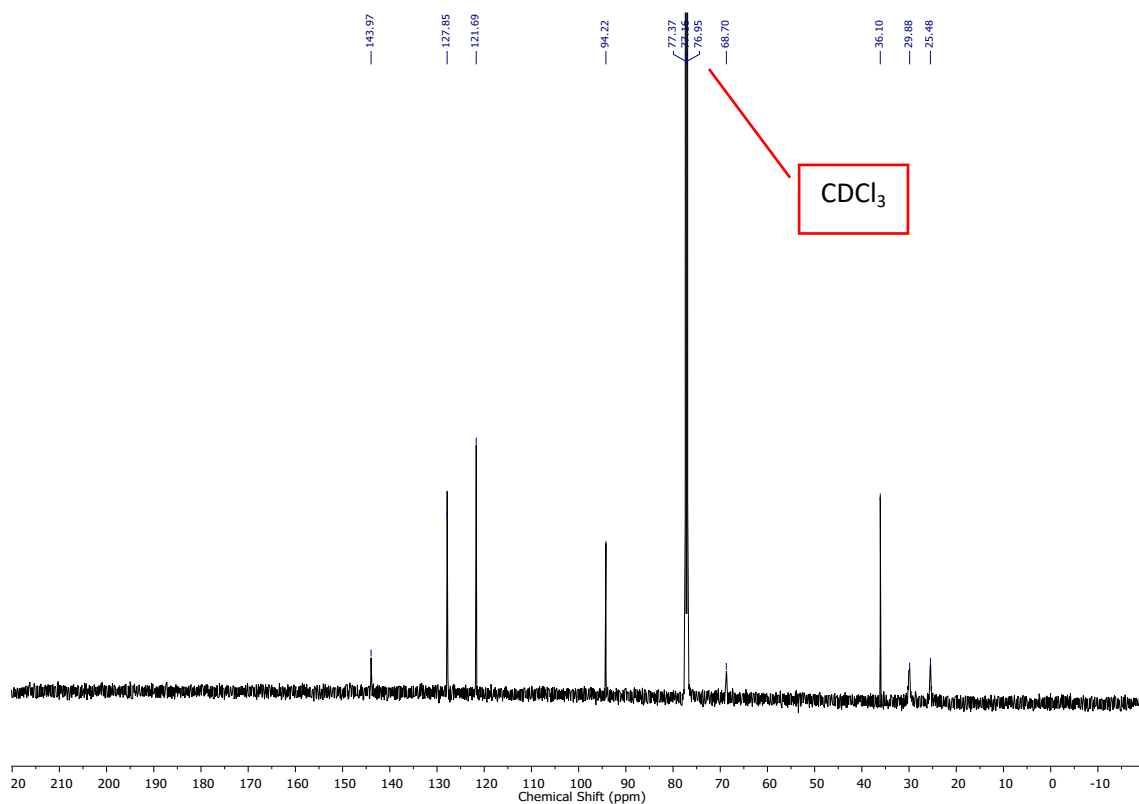


Supplementary Figure 2. ¹³C NMR (150 MHz, CDCl₃) spectrum of 2-methoxy-1,1,3,3-tetramethylisoindoline 2.

1,1,3,3-Tetramethyl-2-((methylsulfinyl)methoxy)isoindoline (3)

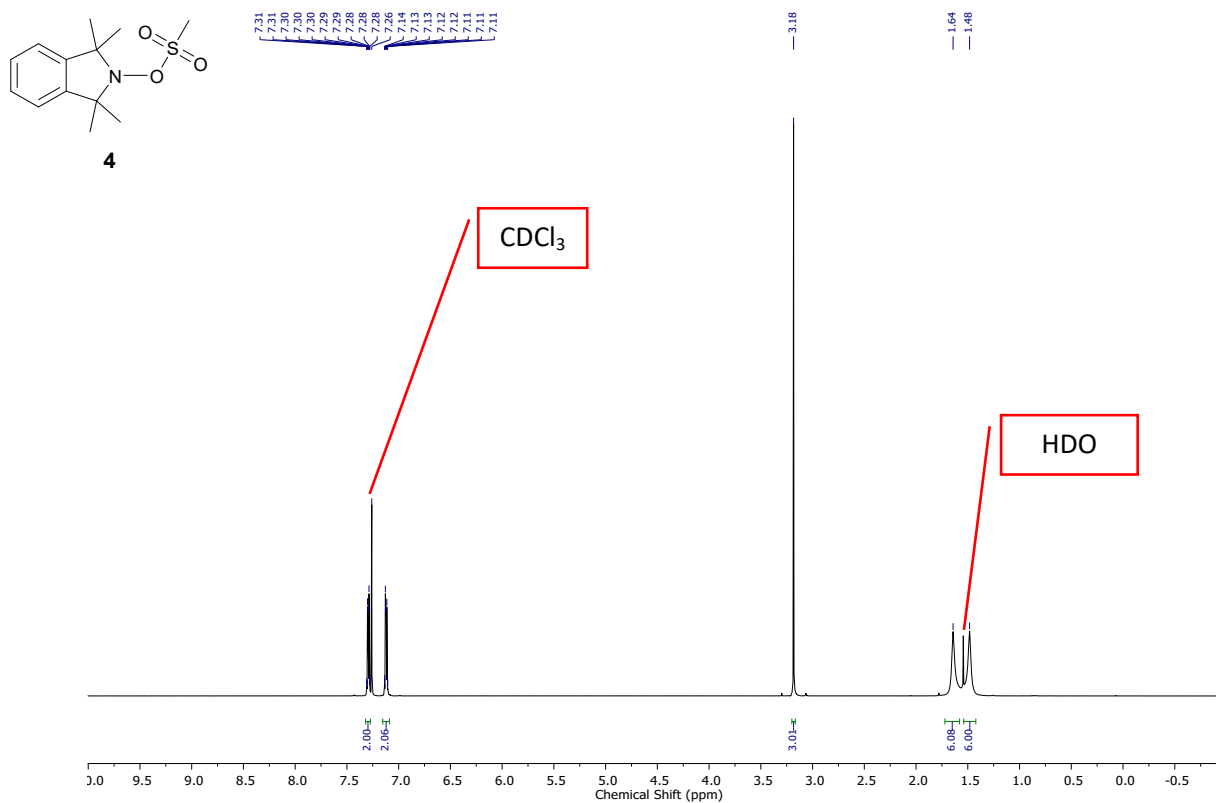


Supplementary Figure 3. ¹H NMR (600 MHz, CDCl₃) spectrum of 1,1,3,3-tetramethyl-2-((methylsulfinyl)methoxy)isoindoline 3.

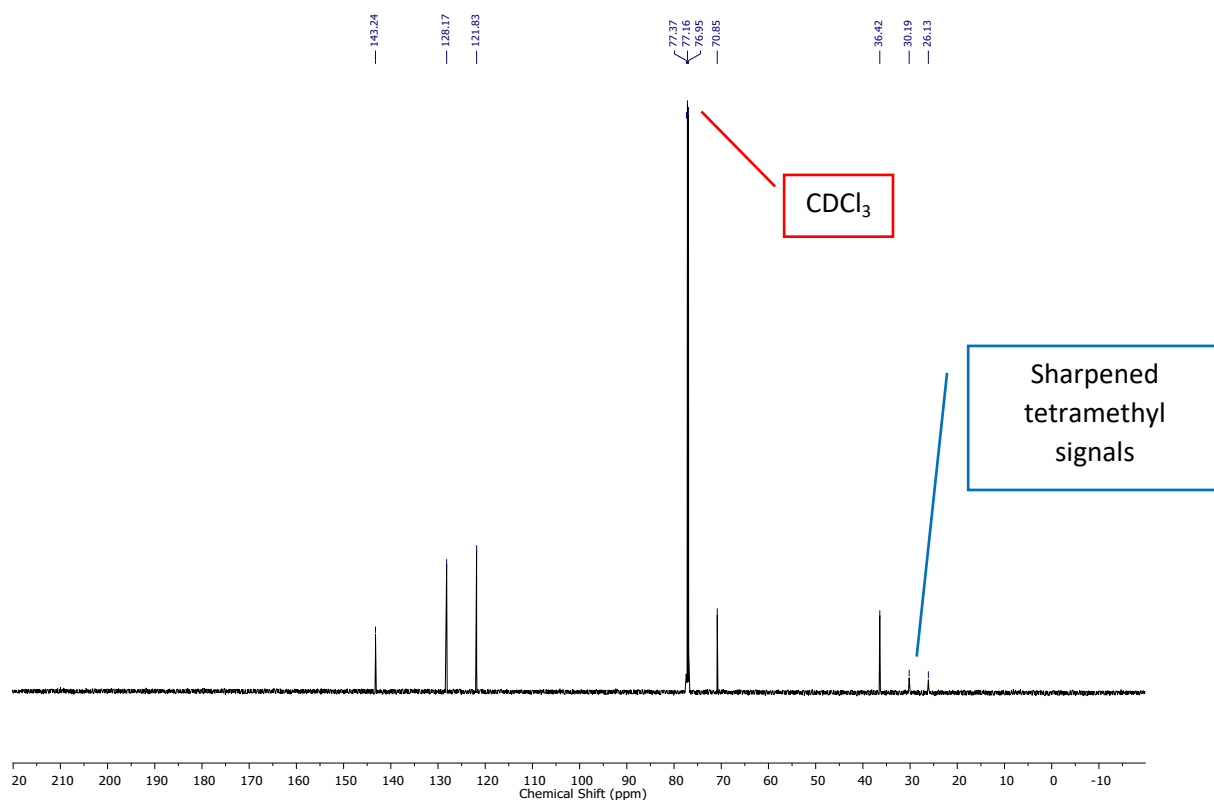


Supplementary Figure 4. ¹³C NMR (150 MHz, CDCl₃) spectrum of 1,1,3,3-tetramethyl-2-((methylsulfinyl)methoxy)isoindoline 3.

1,1,3,3-Tetramethylisoindolin-2-yl methanesulfonate (4)

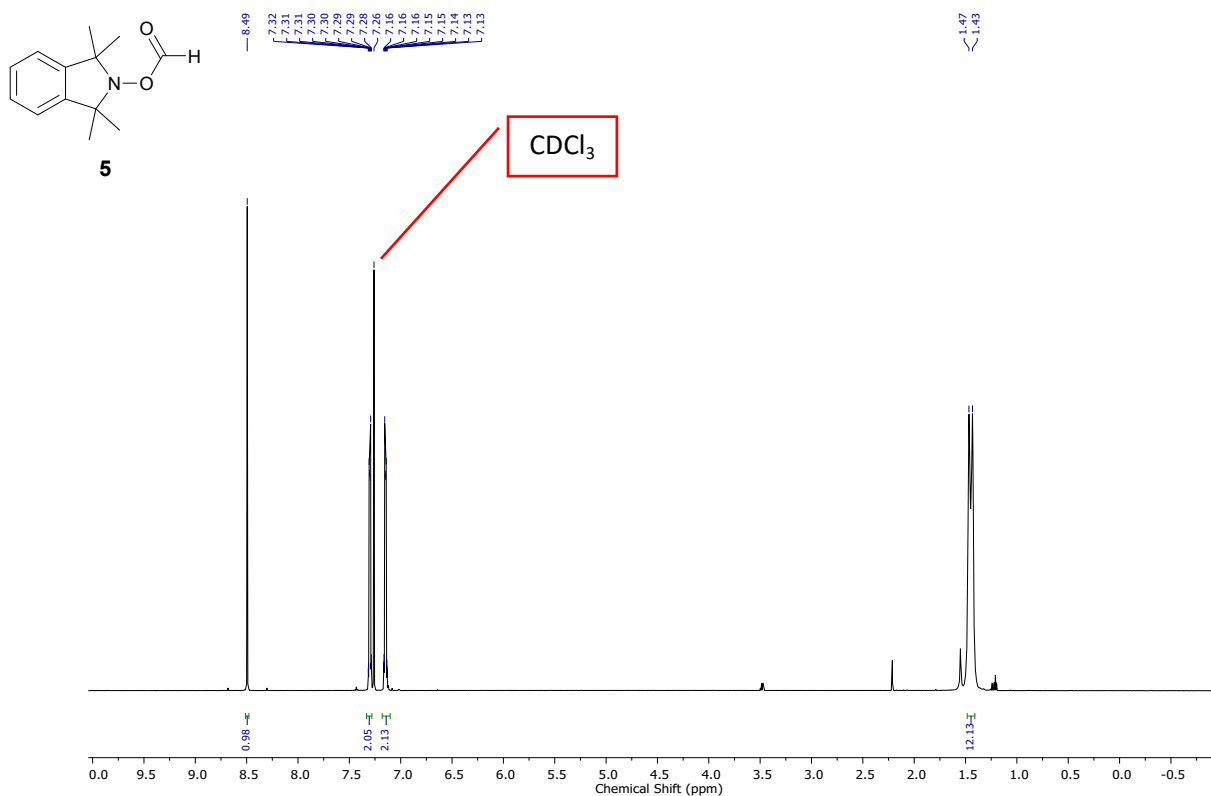


Supplementary Figure 5. ¹H NMR (600 MHz, CDCl₃) spectrum of 1,1,3,3-tetramethylisoindolin-2-yl methanesulfonate 4.

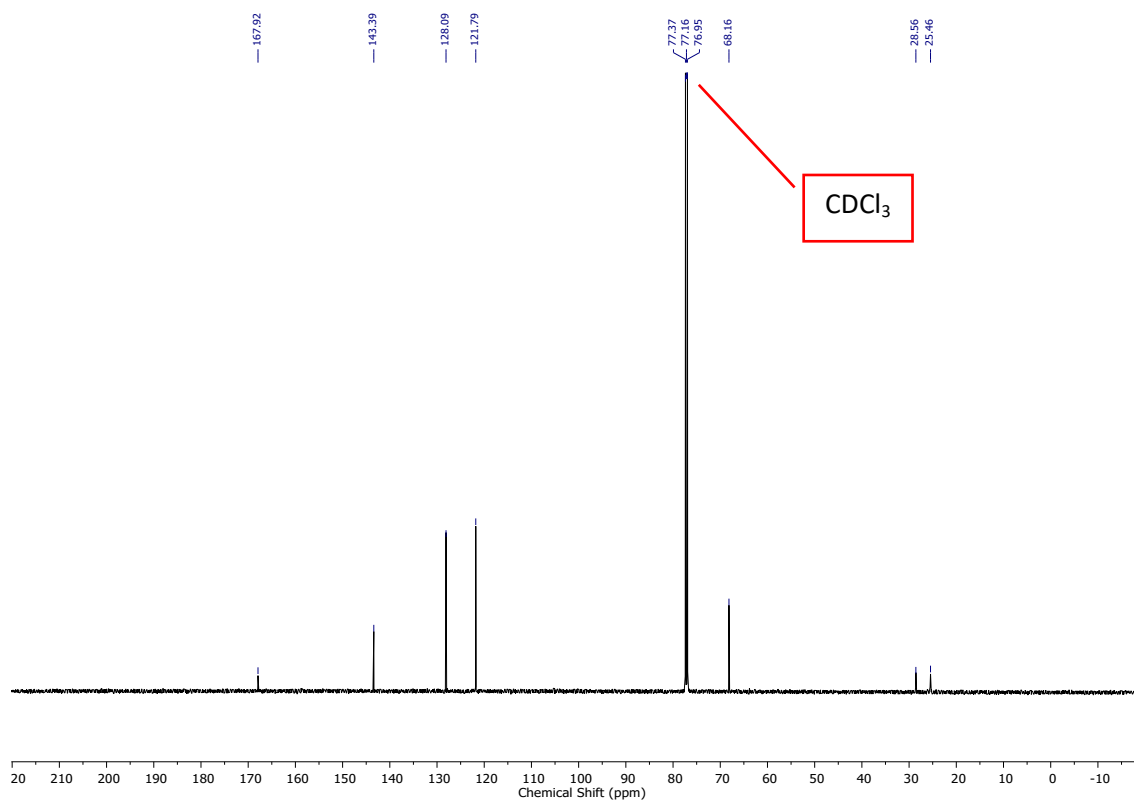


Supplementary Figure 6. ¹³C NMR (150 MHz, CDCl₃) spectrum of 1,1,3,3-tetramethylisoindolin-2-yl methanesulfonate 4.

1,1,3,3-Tetramethylisoindolin-2-yl formate (5)

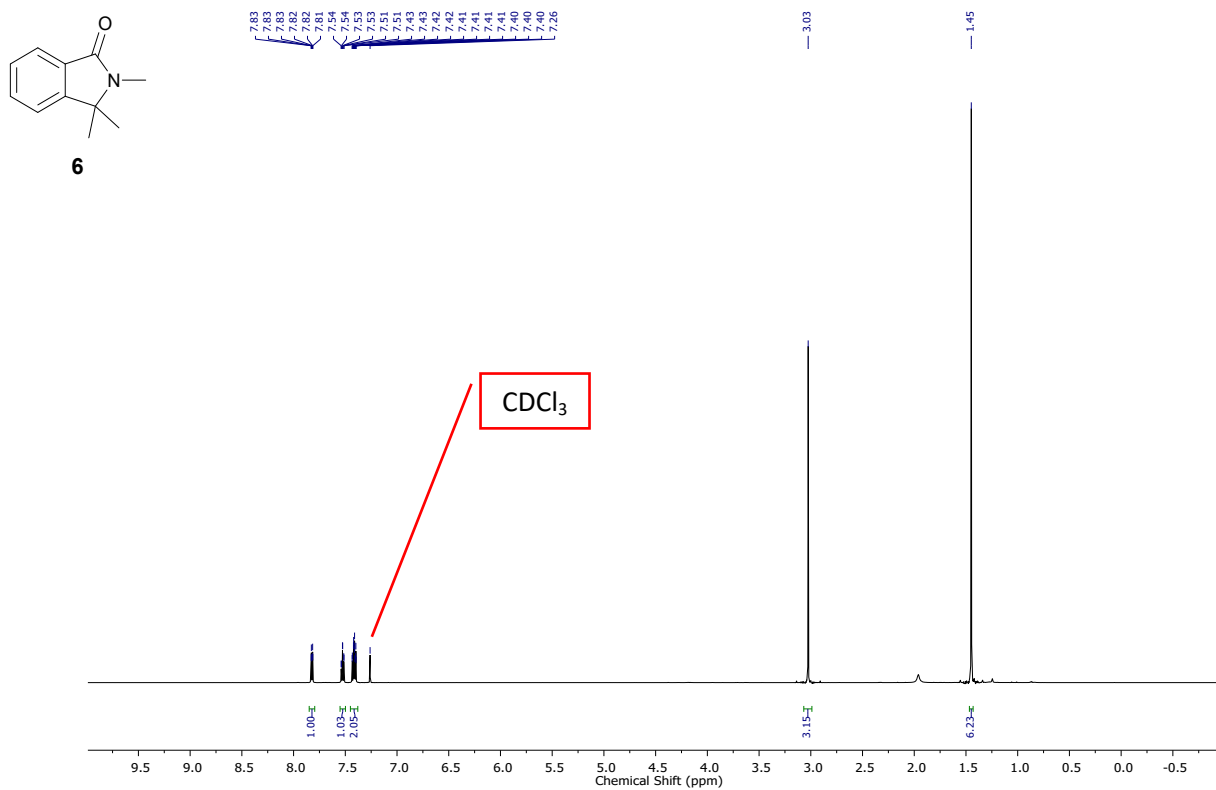


Supplementary Figure 7. ^1H NMR (600 MHz, CDCl_3) spectrum of 1,1,3,3-tetramethylisoindolin-2-yl formate 5.

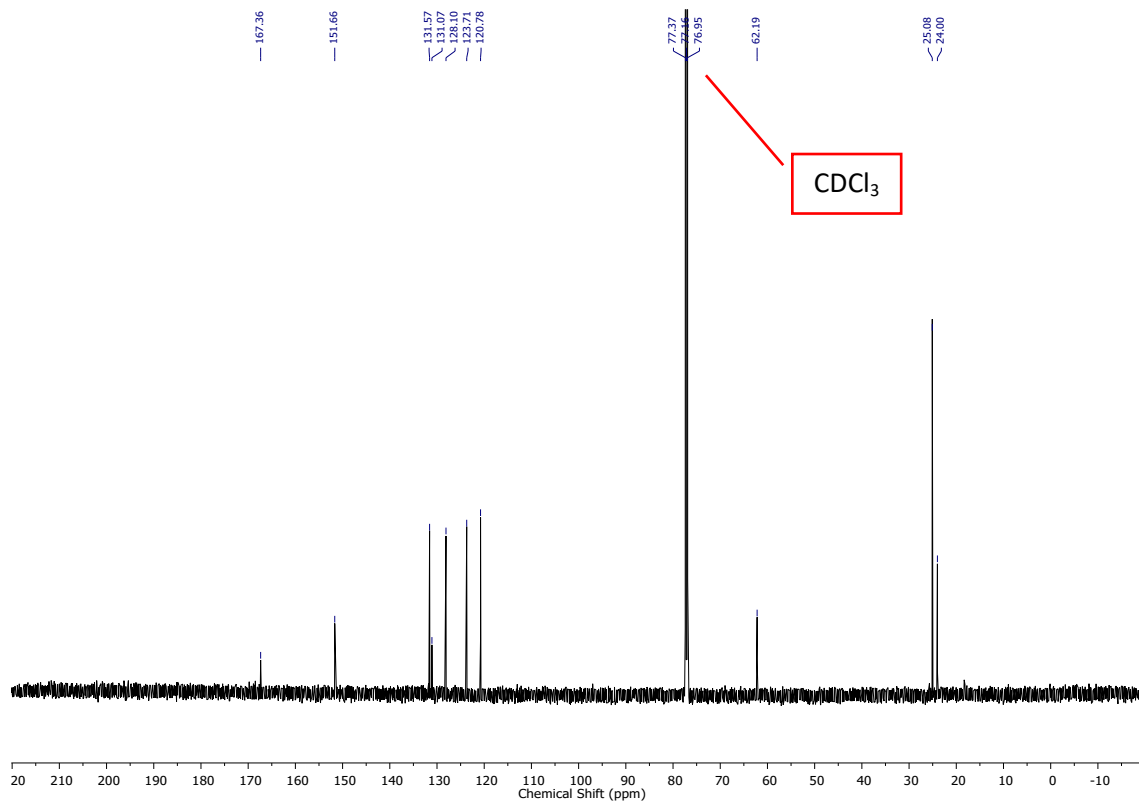


Supplementary Figure 8. ^{13}C NMR (150 MHz, CDCl_3) spectrum of 1,1,3,3-tetramethylisoindolin-2-yl formate 5.

2,3,3-Trimethylisoindolin-1-one (6)

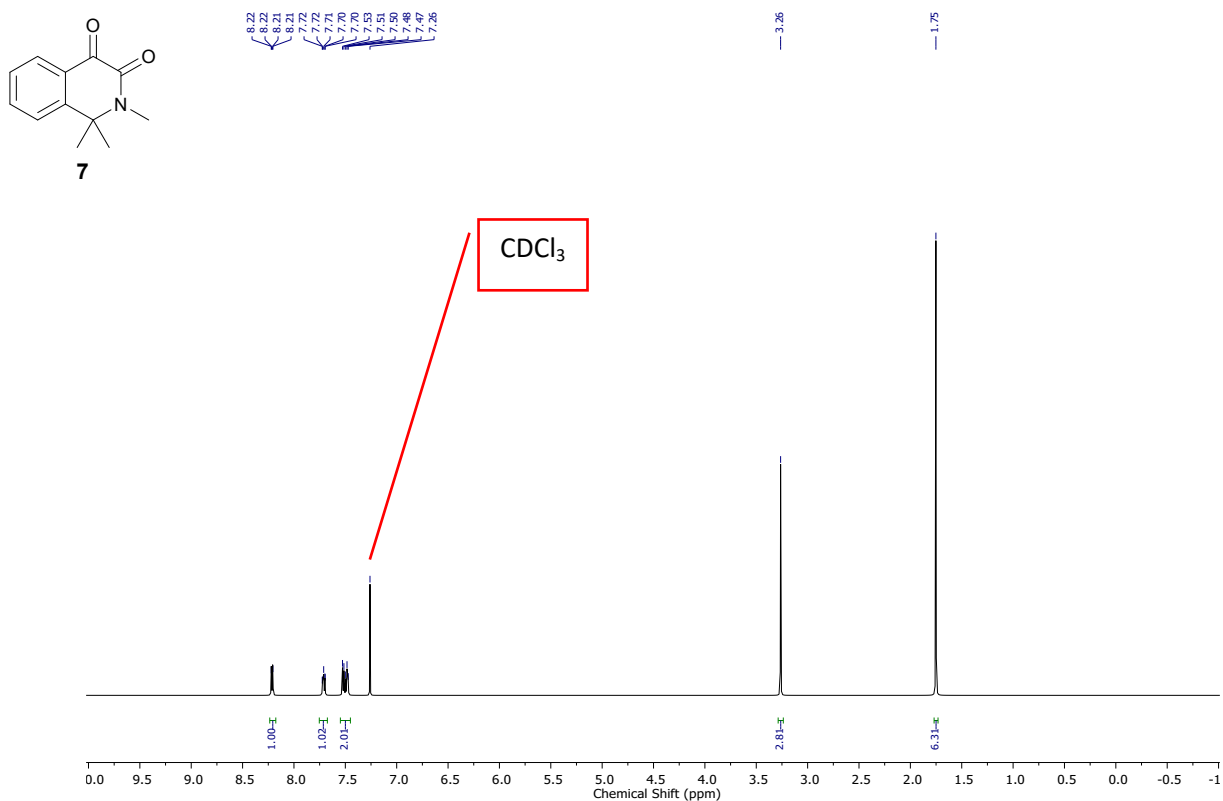


Supplementary Figure 9. ¹H NMR (600 MHz, CDCl₃) spectrum of 2,3,3-trimethylisoindolin-1-one 6.

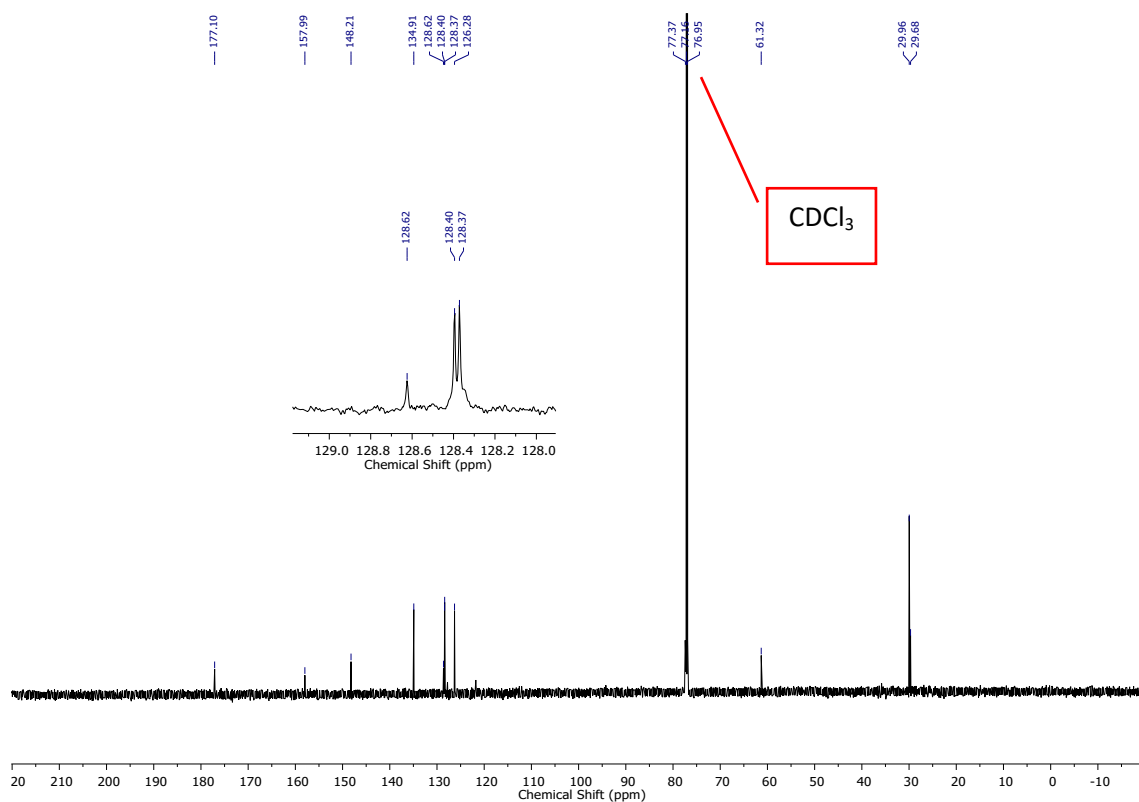


Supplementary Figure 10. ¹³C NMR (150 MHz, CDCl₃) spectrum of 2,3,3-trimethylisoindolin-1-one 6.

1,1,2-Trimethyl-1,2-dihydroisoquinoline-3,4-dione (7)

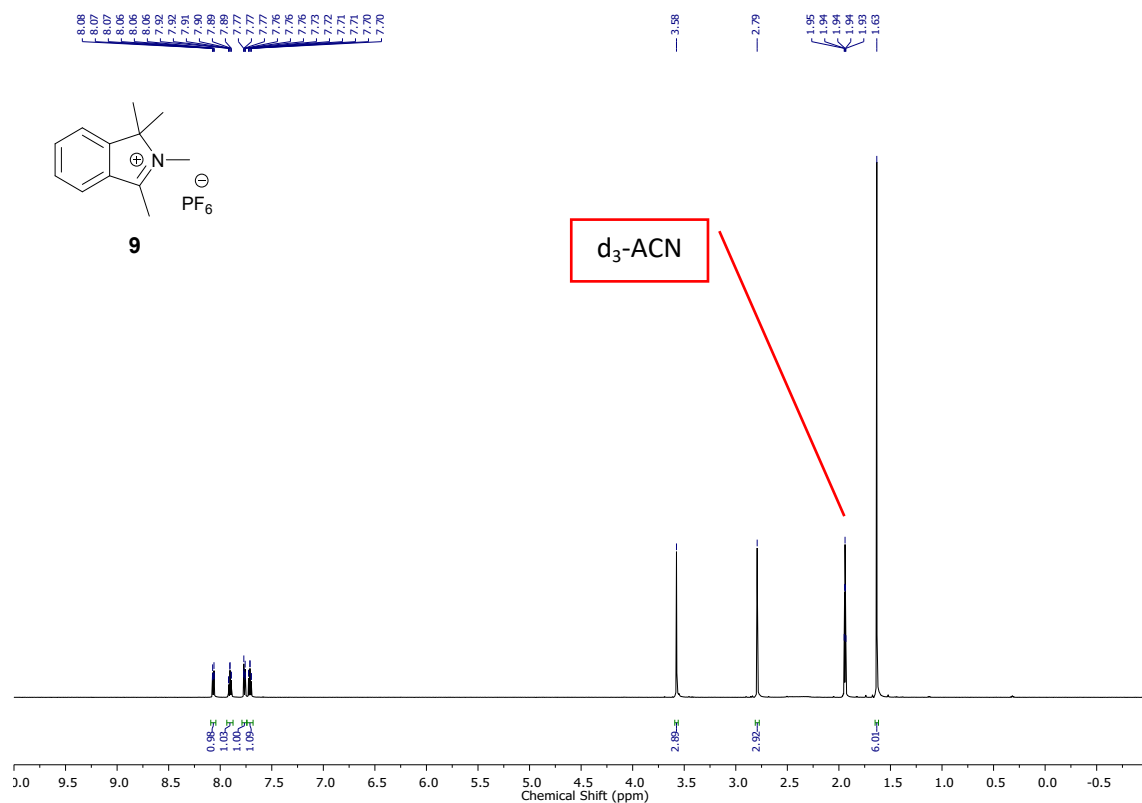


Supplementary Figure 11. ¹H NMR (600 MHz, CDCl₃) spectrum of 1,1,2-trimethyl-1,2-dihydroisoquinoline-3,4-dione 7.

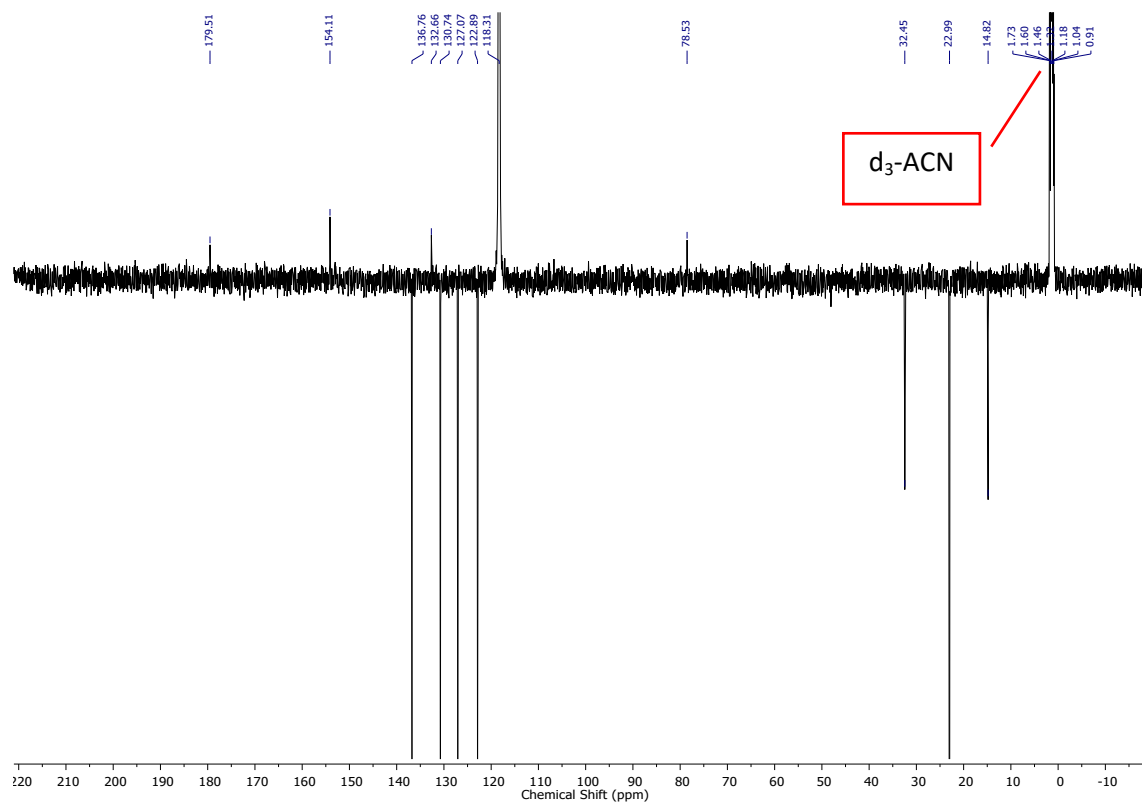


Supplementary Figure 12. ¹³C NMR (150 MHz, CDCl₃) spectrum of 1,1,2-trimethyl-1,2-dihydroisoquinoline-3,4-dione 7.

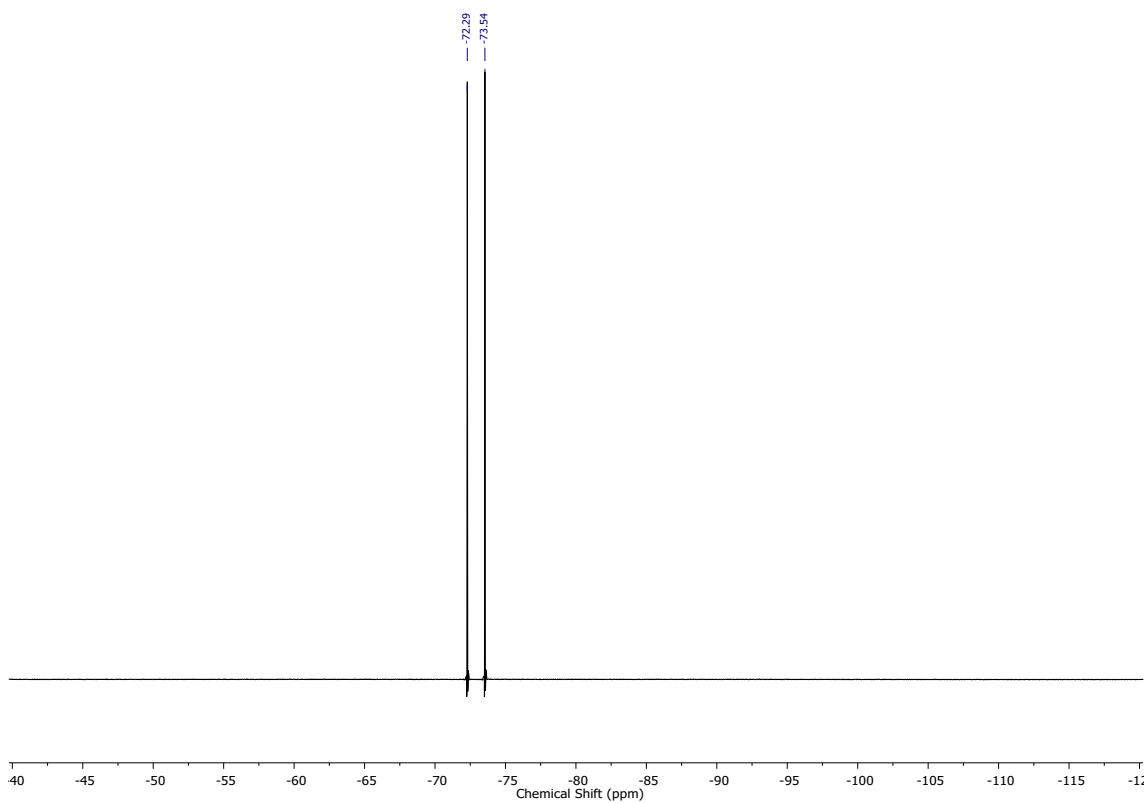
1,1,2,3-Tetramethyl-1H-isoindol-2-ium hexafluorophosphate(V) (9)



Supplementary Figure 13. ¹H NMR (600 MHz, d₃-ACN) spectrum of 1,1,2,3-tetramethyl-1H-isoindol-2-ium hexafluorophosphate(V) 9.

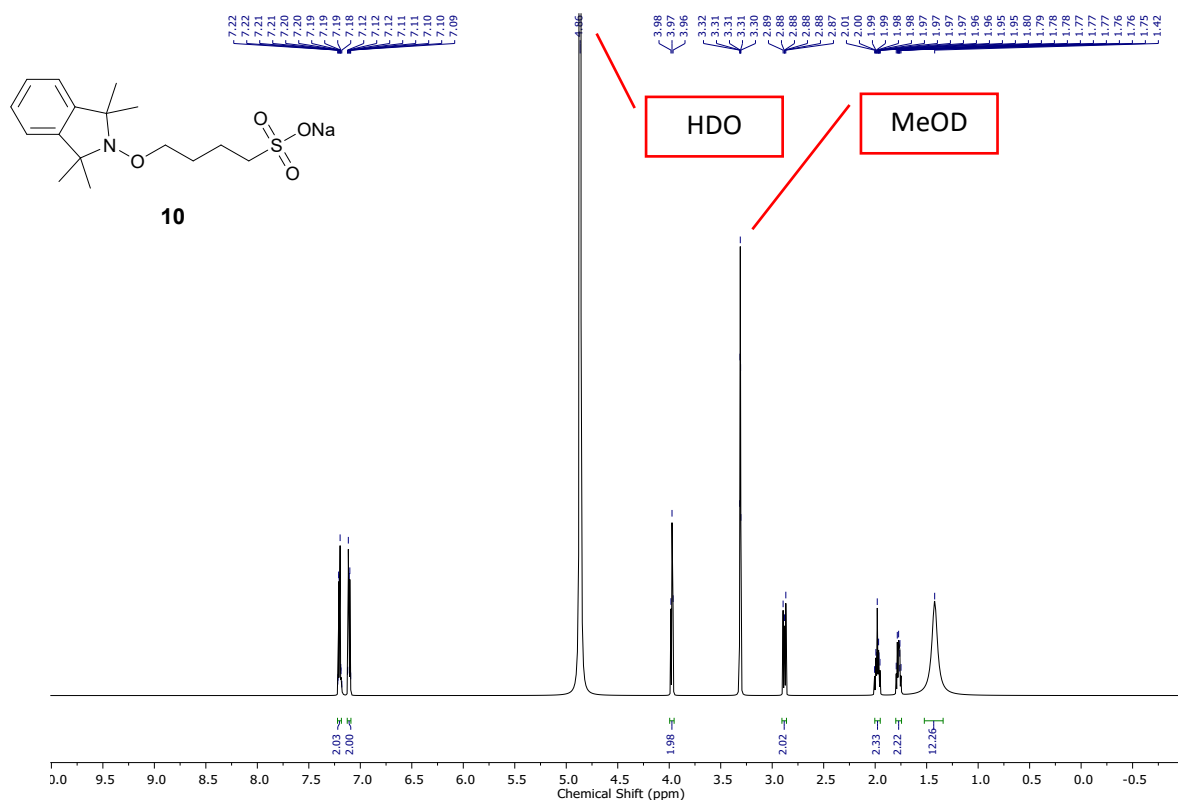


Supplementary Figure 14. ¹³C DEPTQ135 NMR (150 MHz, d₃-ACN) spectrum of 1,1,2,3-tetramethyl-1H-isoindol-2-ium hexafluorophosphate(V) 9.

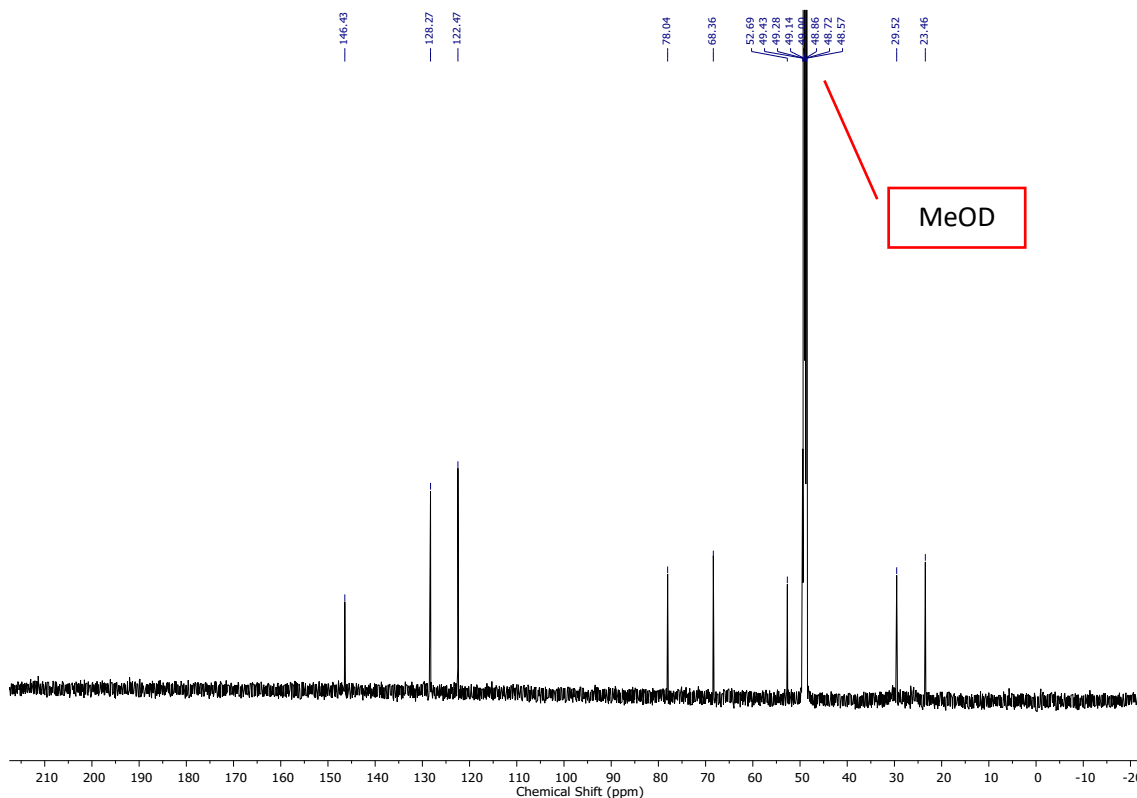


Supplementary Figure 15. ^{19}F NMR (564 MHz, $\text{d}_3\text{-ACN}$) spectrum of 1,1,2,3-tetramethyl-1H-isindol-2-ium hexafluorophosphate(V) **9**.

Sodium 4-((1,1,3,3-tetramethylisoindolin-2-yl)oxy)butane-1-sulfonate (10)

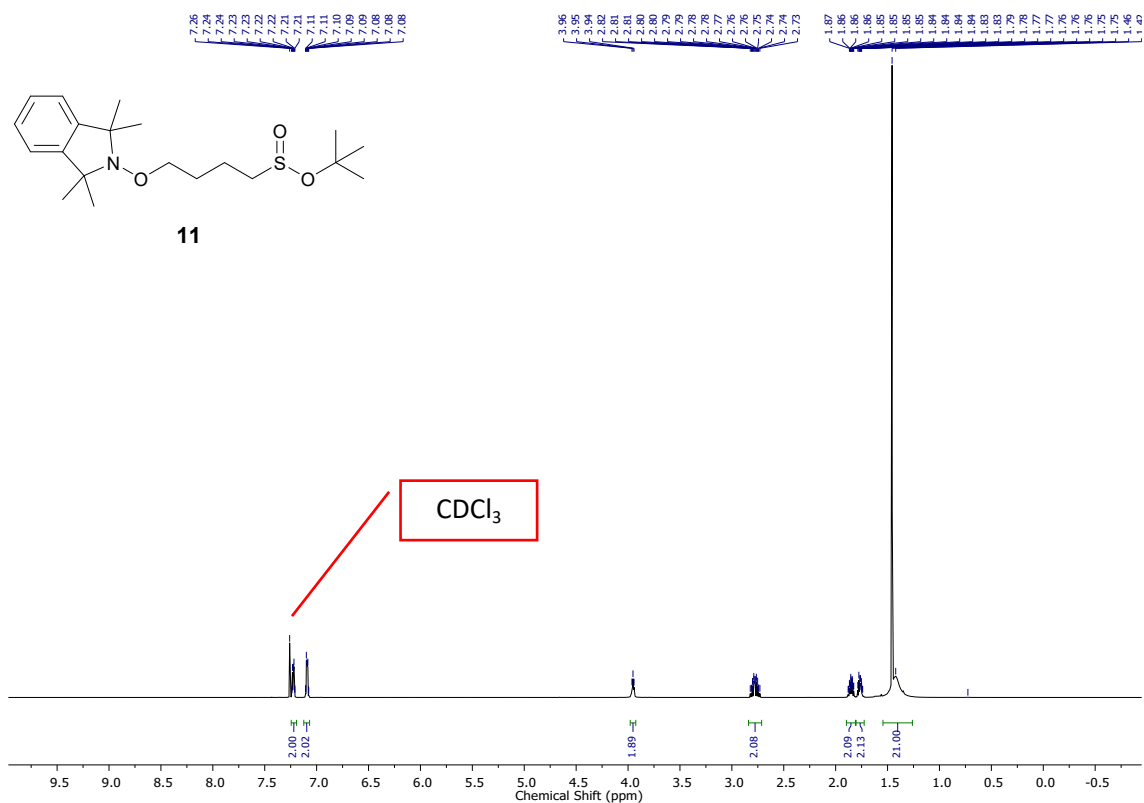


Supplementary Figure 16. ^1H NMR (600 MHz, MeOD) spectrum of sodium 4-((1,1,3,3-tetramethylisoindolin-2-yl)oxy)butane-1-sulfonate **10**.

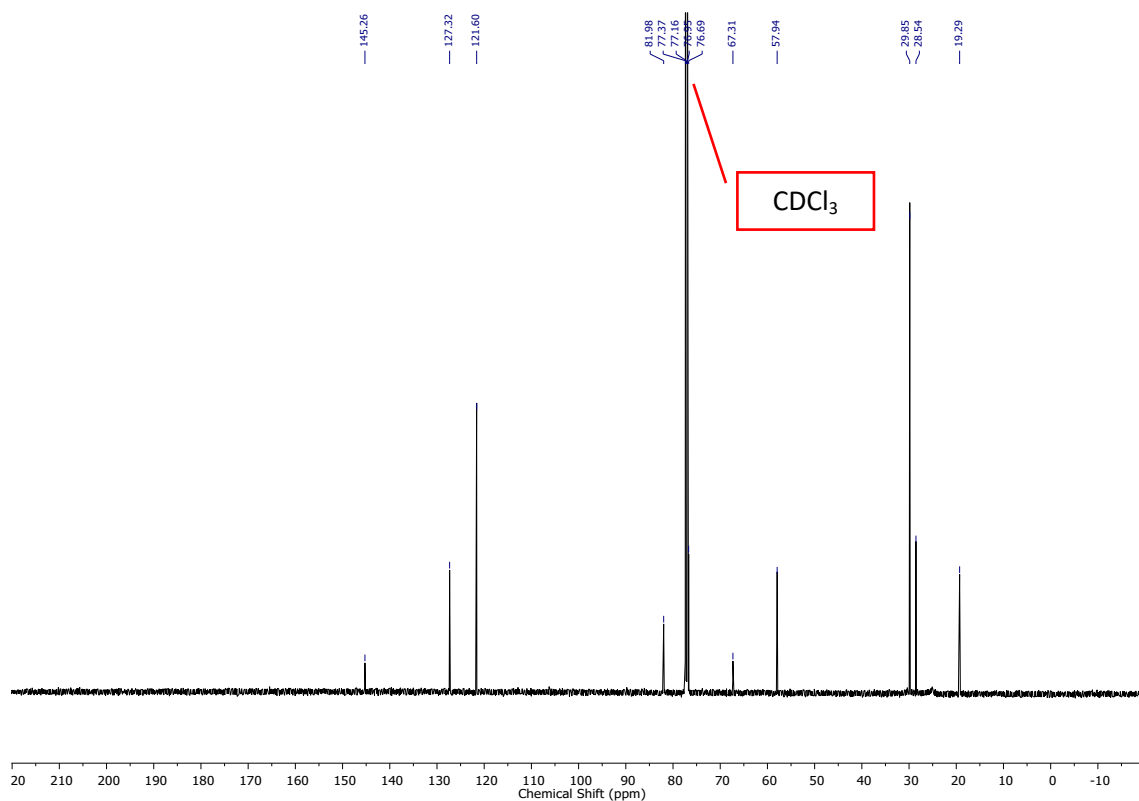


Supplementary Figure 17. ^{13}C NMR (150 MHz, MeOD) spectrum of sodium 4-((1,1,3,3-tetramethylisoindolin-2-yl)oxy)butane-1-sulfonate **10**.

Tert-butyl 4-((1,1,3,3-tetramethylisoindolin-2-yl)oxy)butane-1-sulfinate (11)



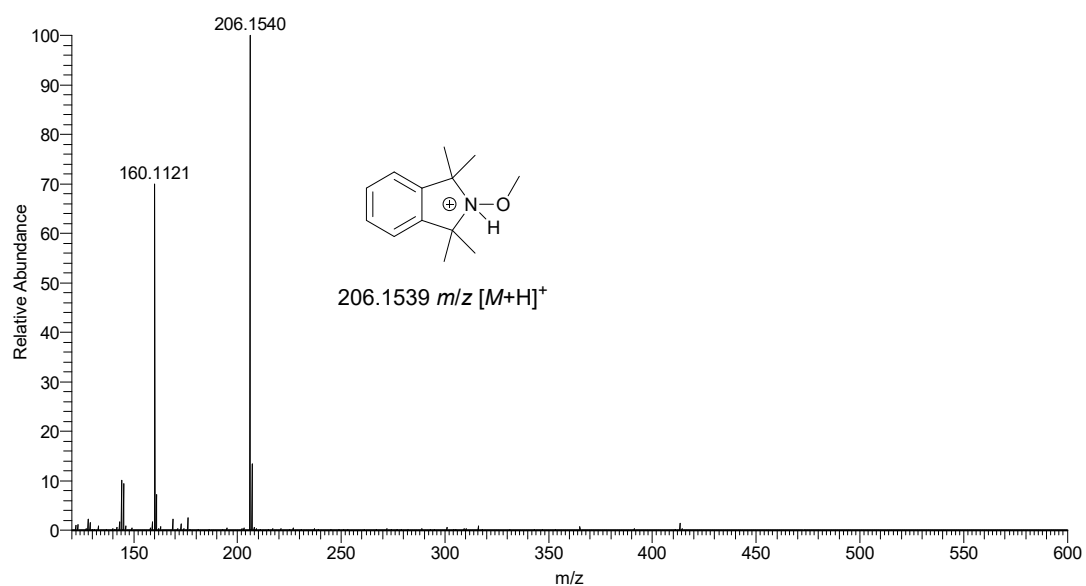
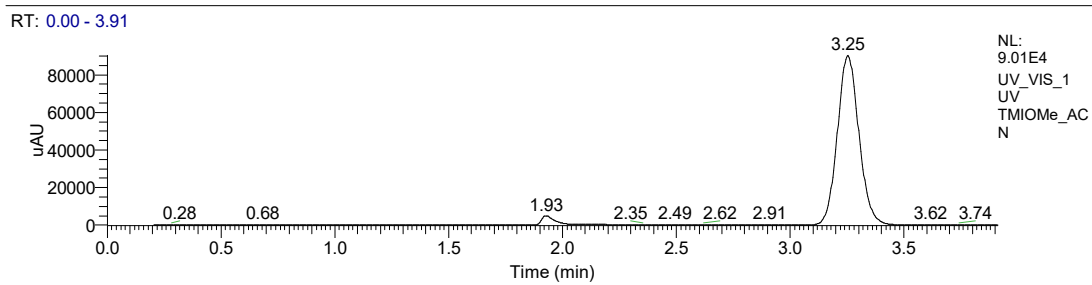
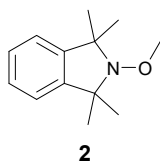
Supplementary Figure 18. ¹H NMR (600 MHz, CDCl₃) spectrum of tert-butyl 4-((1,1,3,3-tetramethylisoindolin-2-yl)oxy)butane-1-sulfinate 11.



Supplementary Figure 19. ¹³C NMR (150 MHz, CDCl₃) spectrum of tert-butyl 4-((1,1,3,3-tetramethylisoindolin-2-yl)oxy)butane-1-sulfinate 11.

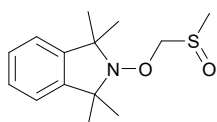
LC-MS Data

2-Methoxy-1,1,3,3-tetramethylisoindoline (2)

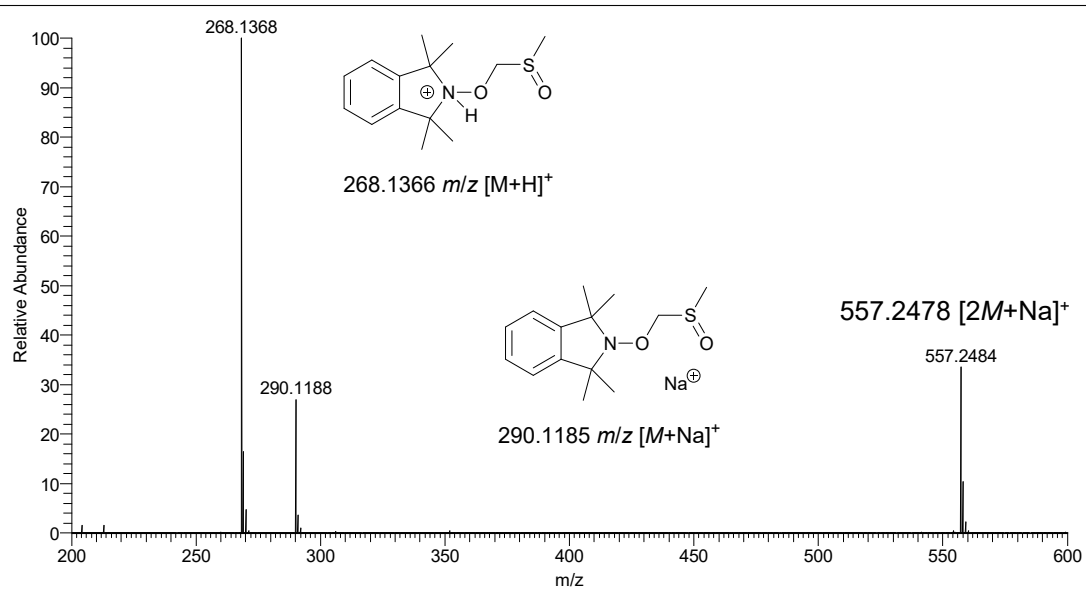
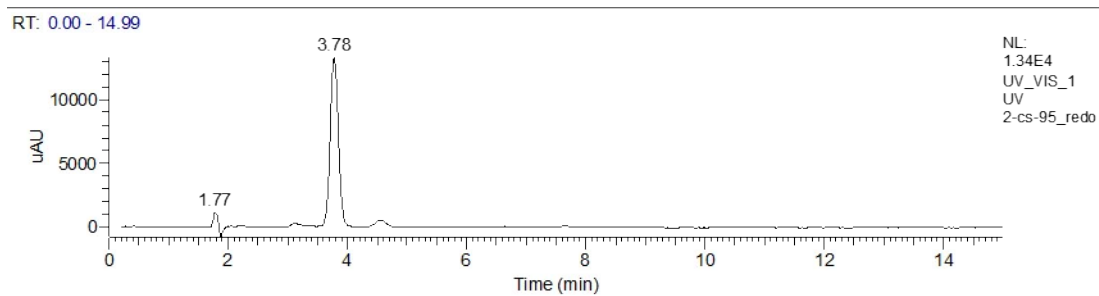


Supplementary Figure 20. LC-MS analysis of 2-methoxy-1,1,3,3-tetramethylisoindoline (2). Solvent A: 100% ACN.

1,1,3,3-Tetramethyl-2-((methylsulfinyl)methoxy)isoindoline (3)

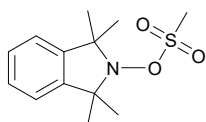


3

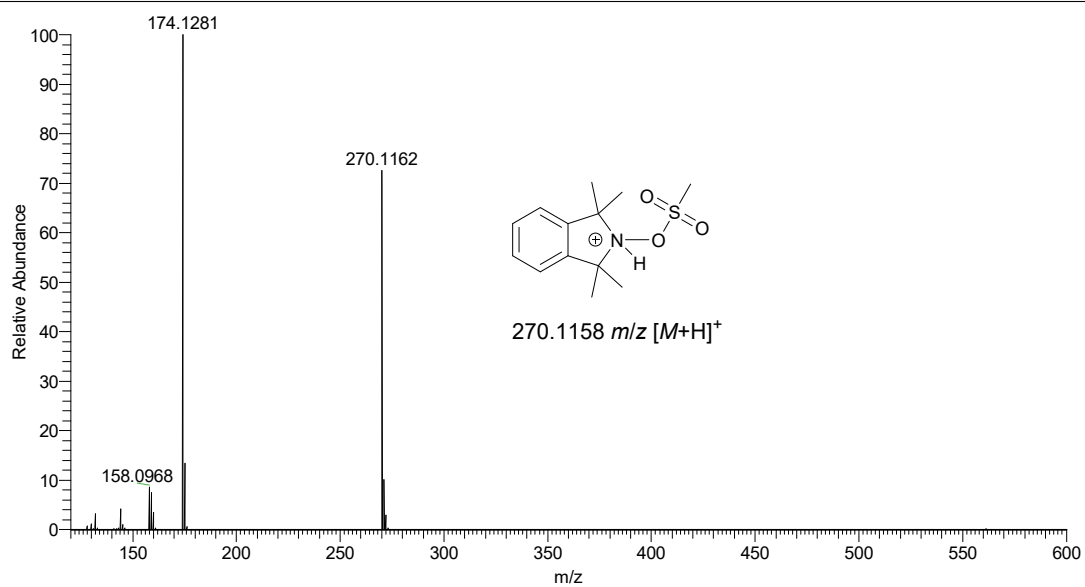
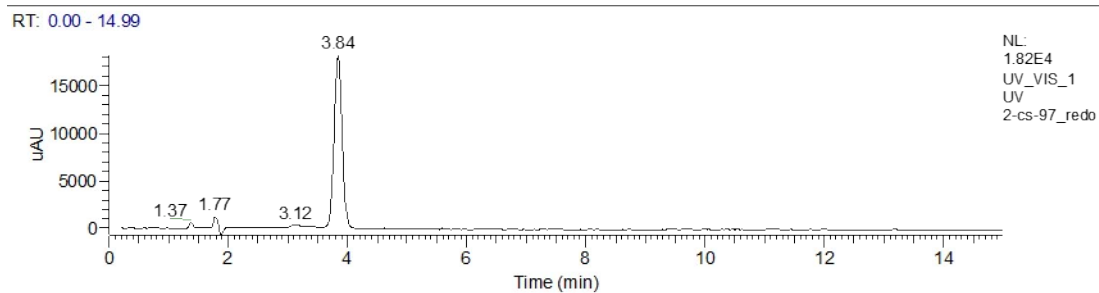


Supplementary Figure 21. LC-MS analysis of 1,1,3,3-tetramethyl-2-((methylsulfinyl)methoxy)isoindoline (3).

1,1,3,3-Tetramethylisoindolin-2-yl methanesulfonate (4)

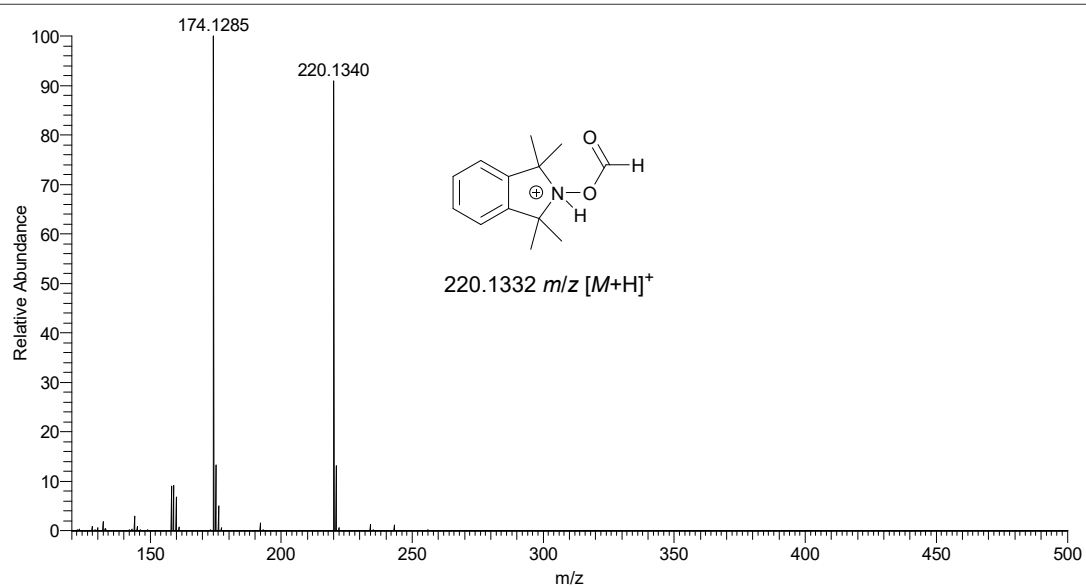
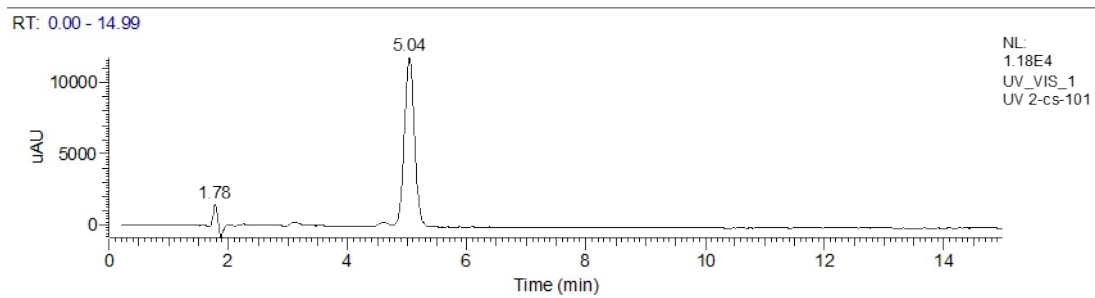
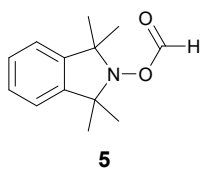


4



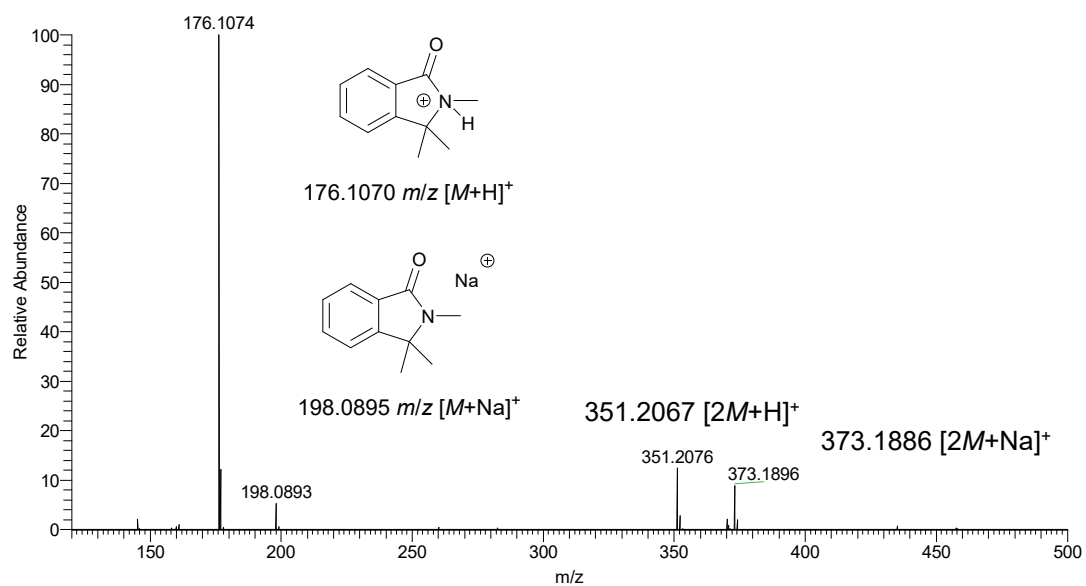
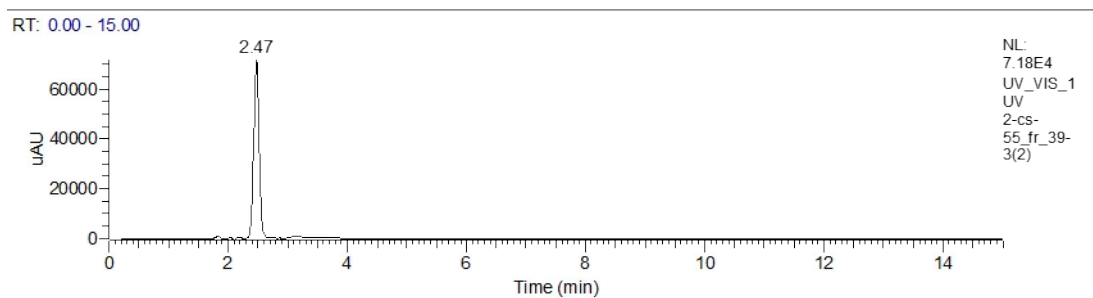
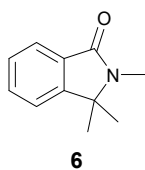
Supplementary Figure 22. LC-MS analysis of 1,1,3,3-tetramethylisoindolin-2-yl methanesulfonate (4).

1,1,3,3-Tetramethylisoindolin-2-yl formate (5)



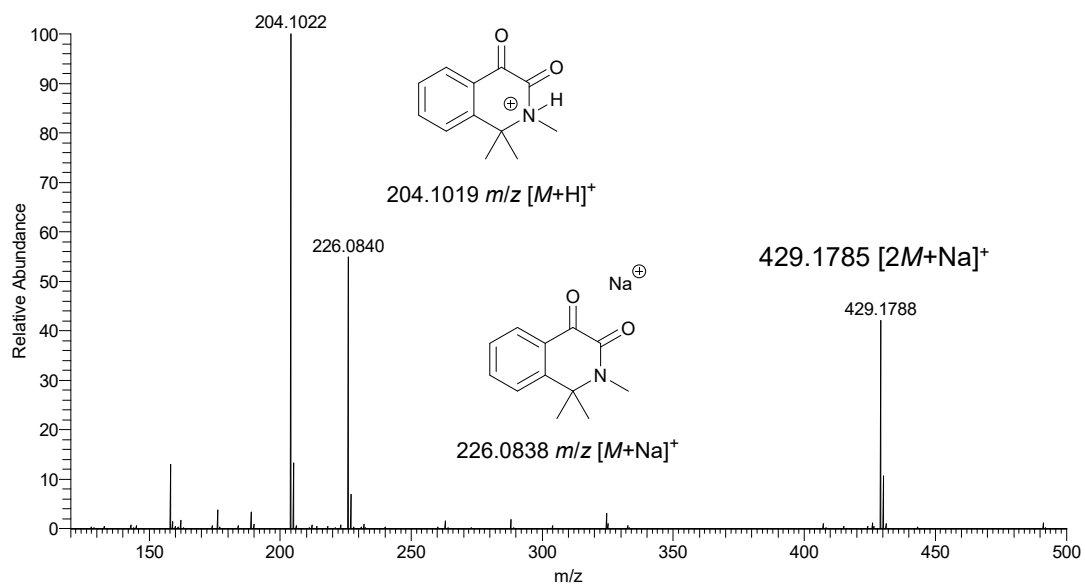
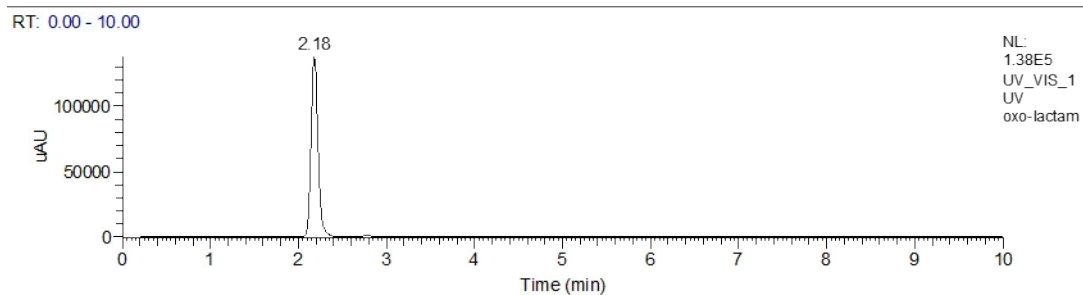
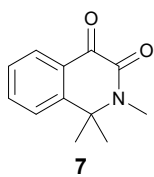
Supplementary Figure 23. LC-MS analysis of 1,1,3,3-tetramethylisoindolin-2-yl formate (5)

2,3,3-Trimethylisoindolin-1-one (6)



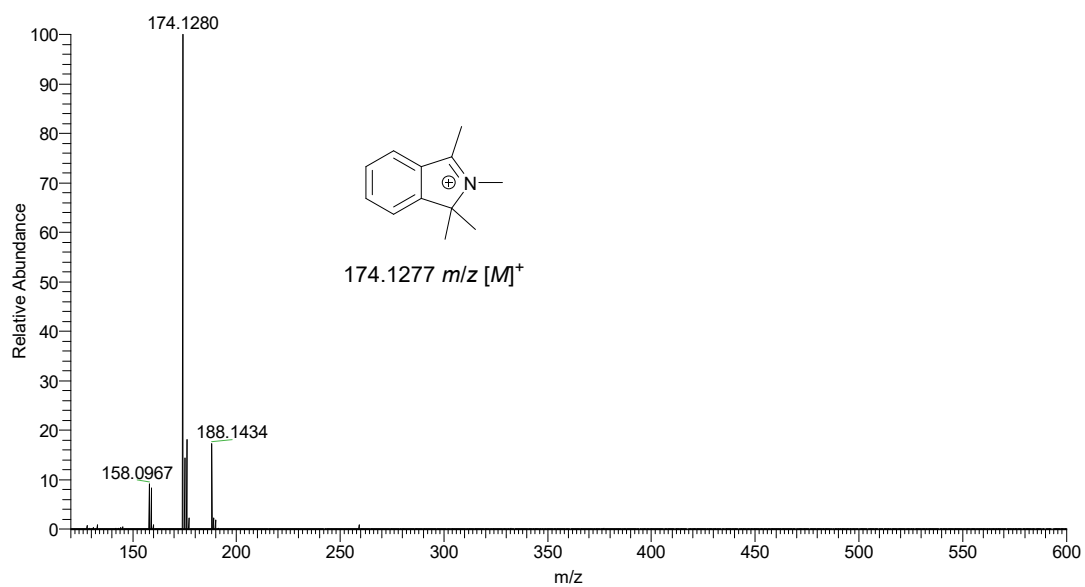
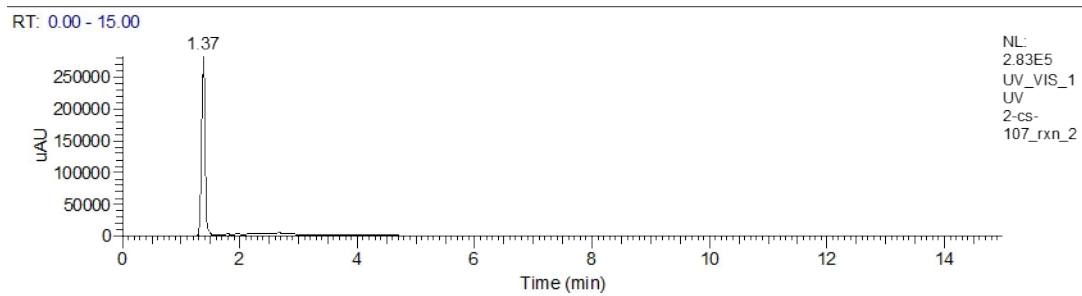
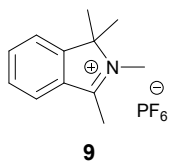
Supplementary Figure 24. LC-MS analysis of 2,3,3-trimethylisoindolin-1-one (6).

1,1,2-Trimethyl-1,2-dihydroisoquinoline-3,4-dione (7)



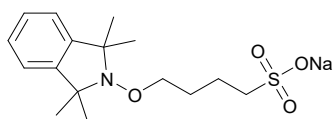
Supplementary Figure 25. LC-MS analysis of 1,1,2-trimethyl-1,2-dihydroisoquinoline-3,4-dione (7).

1,1,2,3-Tetramethyl-1H-isoindol-2-ium hexafluorophosphate(V) (9)

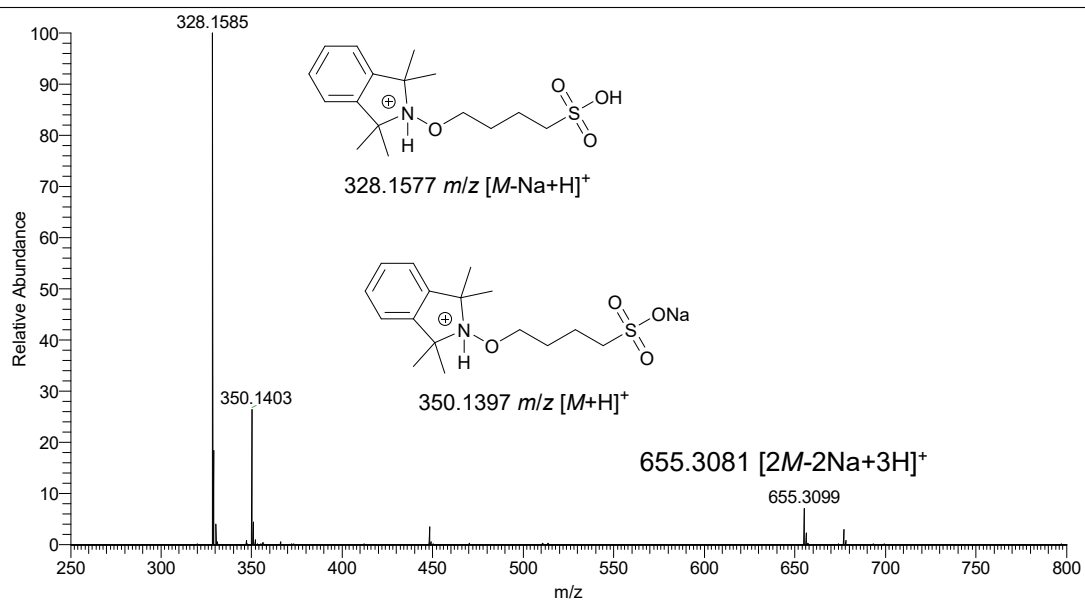
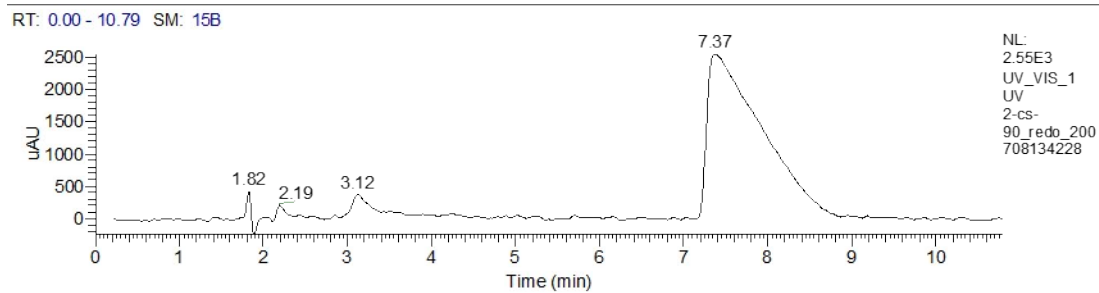


Supplementary Figure 26. LC-MS analysis of 1,1,2,3-tetramethyl-1H-isoindol-2-ium hexafluorophosphate(V) (9).

Sodium 4-((1,1,3,3-tetramethylisindolin-2-yl)oxy)butane-1-sulfonate (10)

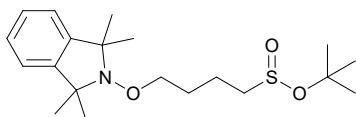


10

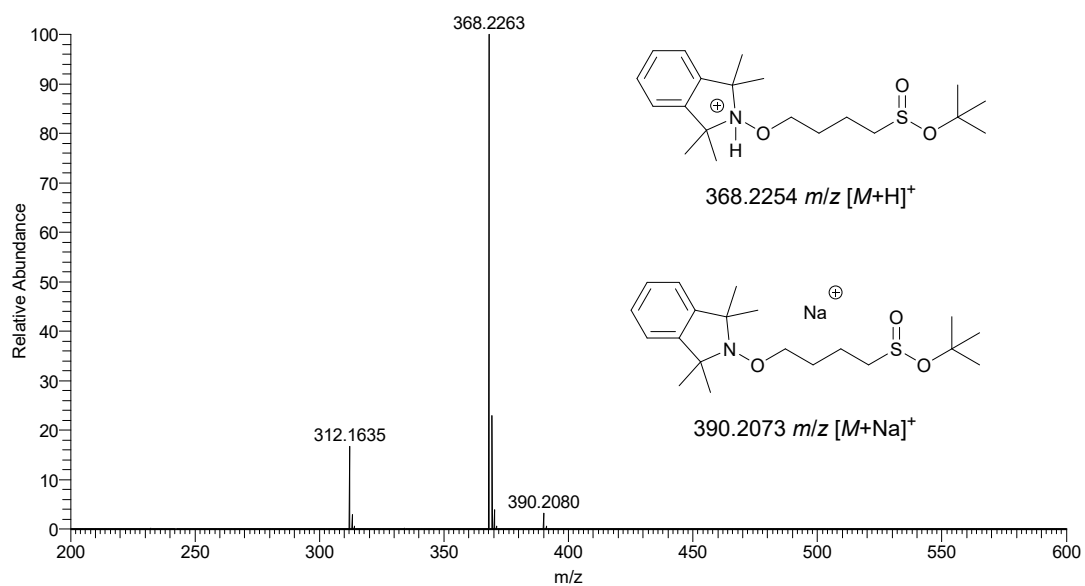
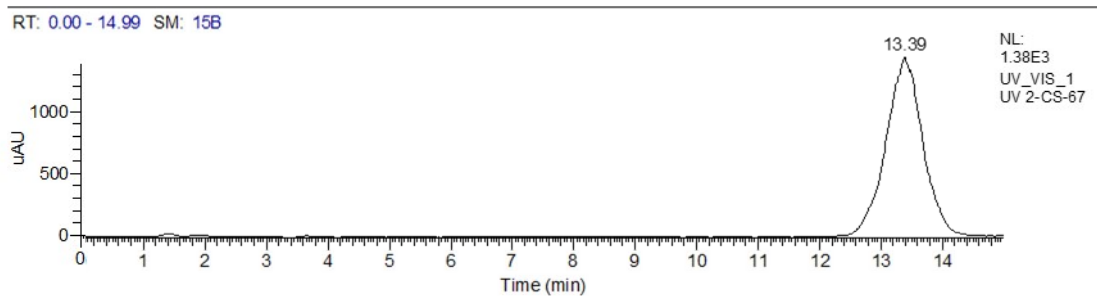


Supplementary Figure 27. LC-MS analysis of sodium 4-((1,1,3,3-tetramethylisindolin-2-yl)oxy)butane-1-sulfonate (10).

Tert-butyl 4-((1,1,3,3-tetramethylisoindolin-2-yl)oxy)butane-1-sulfinate (11)



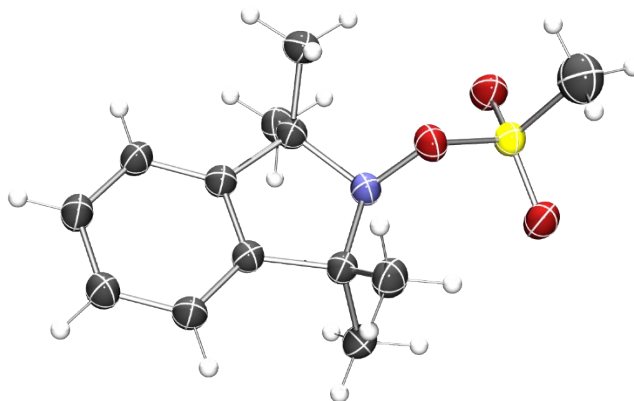
11



Supplementary Figure 28. LC-MS analysis of tert-butyl 4-((1,1,3,3-tetramethylisoindolin-2-yl)oxy)butane-1-sulfinate (11).

Single Crystal XRD of Compounds 4, 5, 7 & 9

1,1,3,3-Tetramethylisoindolin-2-yl methanesulfonate (4)

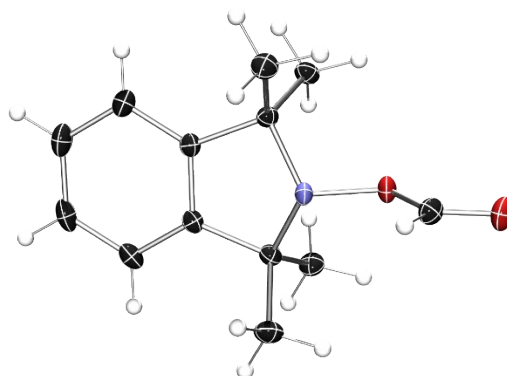


Supplementary Figure 29. ORTEP diagram of crystal structure for 1,1,3,3-tetramethylisoindolin-2-yl methanesulfonate (4). Non-H atoms are shown as anisotropic displacement ellipsoids with 50% probability.

Diffraction data for (4) was collected at 100(2) K on the MX2⁷ beamline at the Australian Synchrotron ($\lambda = 0.7108 \text{ \AA}$). Data was indexed and integrated with XDS⁸. The structure was solved with SHELXT⁹ and refined via a full-matrix least-squares method using SHELXL-2018¹⁰ within the Olex2 graphical interface¹¹. All non-H atoms were refined anisotropically, while H atoms were placed in idealised positions and refined using a riding model on appropriate atoms.

Crystal Data for C₁₃H₁₉NO₃S ($M = 269.35 \text{ g/mol}$): monoclinic, space group P2₁/c (no. 14), $a = 12.307(3) \text{ \AA}$, $b = 10.929(2) \text{ \AA}$, $c = 10.159(2) \text{ \AA}$, $\beta = 90.12(3)^\circ$, $V = 1366.4(5) \text{ \AA}^3$, $Z = 4$, $T = 100.0 \text{ K}$, $\mu(\text{Synchrotron}) = 0.237 \text{ mm}^{-1}$, $D_{\text{calc}} = 1.309 \text{ g/cm}^3$, 18820 reflections measured ($3.31^\circ \leq 2\theta \leq 54.198^\circ$), 2866 unique ($R_{\text{int}} = 0.0935$, $R_{\text{sigma}} = 0.0578$) which were used in all calculations. The final R_1 was 0.0650 ($I > 2\sigma(I)$) and wR_2 was 0.2008 (all data).

1,1,3,3-Tetramethylisoindolin-2-yl formate (5)

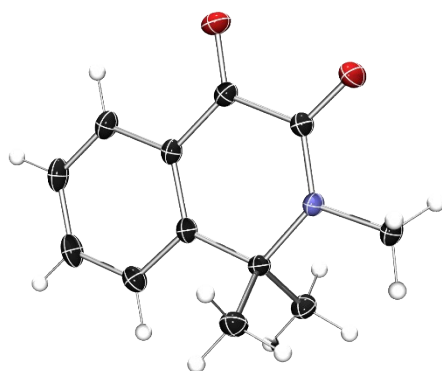


Supplementary Figure 30. ORTEP diagram of crystal structure for 1,1,3,3-tetramethylisoindolin-2-yl formate (5). Non-H atoms are shown as anisotropic displacement ellipsoids with 50% probability.

Diffraction data for (5) was collected at 100(2) K on the MX1 beamline¹² at the Australian Synchrotron ($\lambda = 0.7108 \text{ \AA}$). Data was indexed and integrated with XDS⁸. The structure was solved with SHELXT⁹ and refined via a full-matrix least-squares method using SHELXL-2018¹⁰ within the Olex2 graphical interface¹¹. All non-H atoms were refined anisotropically, while H atoms were placed in idealised positions and refined using a riding model on appropriate atoms.

Crystal Data for $C_{13}H_{17}NO_2$ ($M = 219.27 \text{ g/mol}$): orthorhombic, space group $Pna2_1$ (no. 33), $a = 11.509(2) \text{ \AA}$, $b = 14.815(3) \text{ \AA}$, $c = 7.0560(14) \text{ \AA}$, $V = 1203.1(4) \text{ \AA}^3$, $Z = 4$, $T = 100(2) \text{ K}$, $\mu(\text{Synchrotron}) = 0.081 \text{ mm}^{-1}$, $D_{\text{calc}} = 1.211 \text{ g/cm}^3$, 15914 reflections measured ($4.482^\circ \leq 2\theta \leq 59.012^\circ$), 2881 unique ($R_{\text{int}} = 0.0681$, $R_{\text{sigma}} = 0.0429$) which were used in all calculations. The final R_1 was 0.0343 ($I > 2\sigma(I)$) and wR_2 was 0.0919 (all data).

1,1,2-Trimethyl-1,2-dihydroisoquinoline-3,4-dione (7)

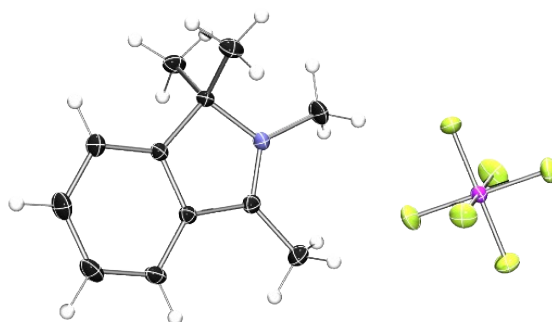


Supplementary Figure 31. ORTEP diagram of the crystal structure of 1,1,2-trimethyl-1,2-dihydroisoquinoline-3,4-dione (7). Non-H atoms are shown as anisotropic displacement ellipsoids with 50% probability.

Diffraction data for (7) was collected at 100(2) K on the MX1 beamline¹² at the Australian Synchrotron ($\lambda = 0.7109 \text{ \AA}$). Data was indexed and integrated with XDS⁸. The structure was solved with SHELXT⁹ and refined via a full-matrix least-squares method using SHELXL-2018¹⁰ within the Olex2 graphical interface¹¹. All non-H atoms were refined anisotropically, while H atoms were placed in idealised positions and refined using a riding model on appropriate atoms.

Crystal Data for $C_{12}H_{13}NO_2$ ($M = 203.23 \text{ g/mol}$): monoclinic, space group $P2_1/m$ (no. 11), $a = 7.9850(16) \text{ \AA}$, $b = 6.6850(13) \text{ \AA}$, $c = 9.4400(19) \text{ \AA}$, $\beta = 100.86(3)^\circ$, $V = 494.88(18) \text{ \AA}^3$, $Z = 2$, $T = 100(2) \text{ K}$, $\mu(\text{Synchrotron}) = 0.093 \text{ mm}^{-1}$, $D_{\text{calc}} = 1.364 \text{ g/cm}^3$, 6912 reflections measured ($4.394^\circ \leq 2\theta \leq 58.656^\circ$), 1144 unique ($R_{\text{int}} = 0.0418$, $R_{\text{sigma}} = 0.0282$) which were used in all calculations. The final R_1 was 0.0372 ($I > 2\sigma(I)$) and wR_2 was 0.1126 (all data).

1,1,2,3-Tetramethyl-1H-isoindol-2-ium hexafluorophosphate(V) (9)



Supplementary Figure 32. ORTEP diagram of the crystal structure of 1,1,2,3-tetramethyl-1H-isoindol-2-ium hexafluorophosphate(V) (9). Non-H atoms are shown as anisotropic displacement ellipsoids with 50% probability.

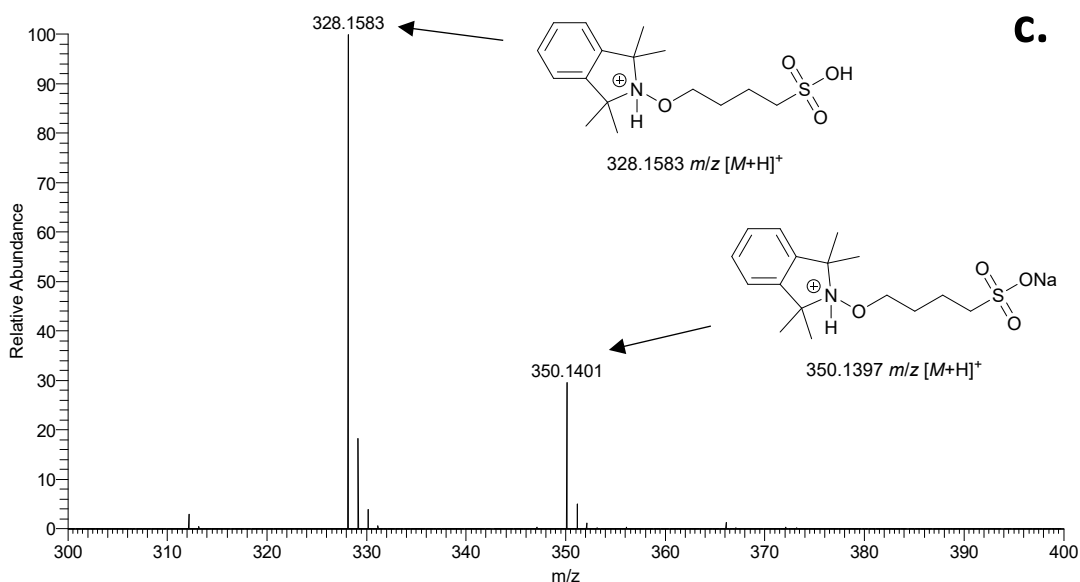
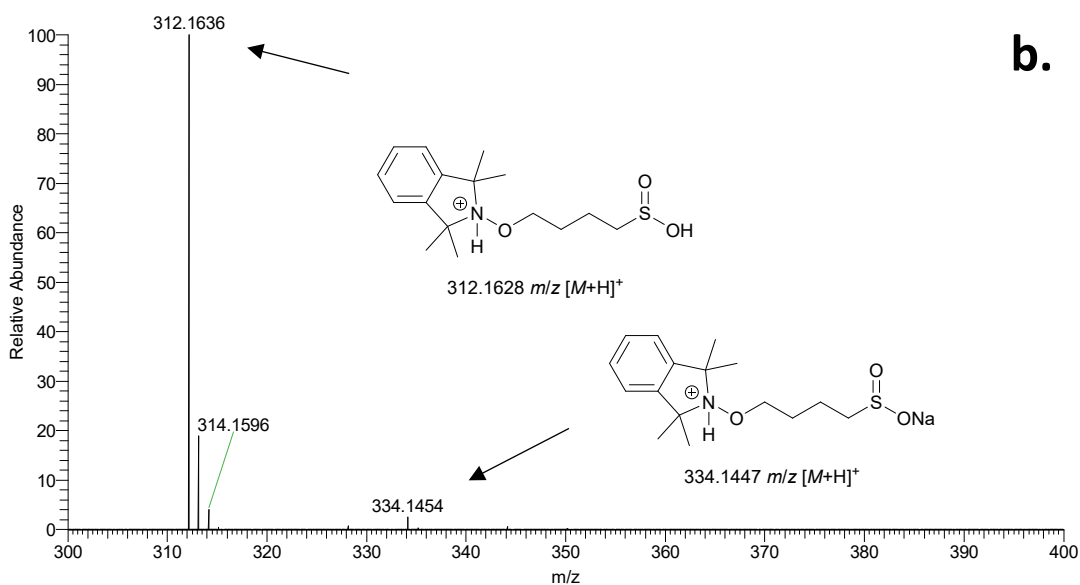
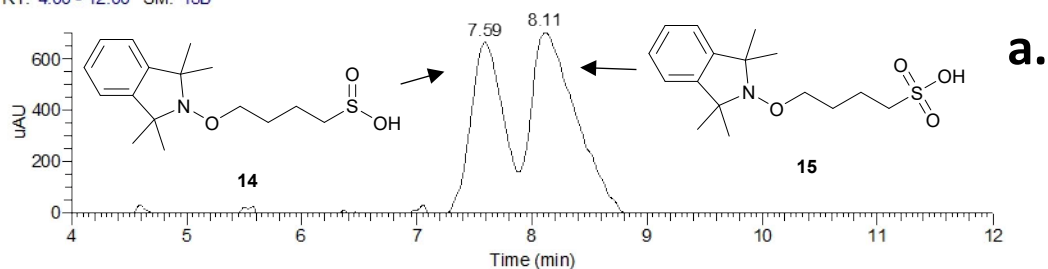
Diffraction data for (9) was collected at 100.1(2) K on a Rigaku XtaLAB Synergy Dualflex diffractometer equipped with Pilatus 300K detector using micro-focused mirror-collimated X-rays ($\lambda = \text{Ag K}\alpha$, 0.56087 Å) generated from a sealed tube (PhotonJet Ag). Data indexation, reduction and integration was conducted within CrysAlis Pro¹³. The structure was solved with SHELXT⁹ and refined via a full-matrix least-squares method using SHELXL-2018¹⁰ within the Olex2 graphical interface¹¹. All non-H atoms were refined anisotropically, while H atoms were placed in idealised positions and refined using a riding model on appropriate atoms.

Crystal Data for $\text{C}_{12}\text{H}_{16}\text{F}_6\text{NP}$ ($M = 319.23$ g/mol): monoclinic, space group I2/a (no. 15), $a = 18.8169(6)$ Å, $b = 6.4663(2)$ Å, $c = 22.5305(7)$ Å, $\beta = 96.669(3)^\circ$, $V = 2722.87(15)$ Å³, $Z = 8$, $T = 100.1(2)$ K, $\mu(\text{Ag K}\alpha) = 0.142$ mm⁻¹, $D_{\text{calc}} = 1.557$ g/cm³, 19340 reflections measured ($4.73^\circ \leq 2\theta \leq 44.538^\circ$), 3518 unique ($R_{\text{int}} = 0.0603$, $R_{\text{sigma}} = 0.0447$) which were used in all calculations. The final R_1 was 0.0372 ($I > 2\sigma(I)$) and wR_2 was 0.1073 (all data).

Characterisation Data for Non-Isolated Products (12-15)

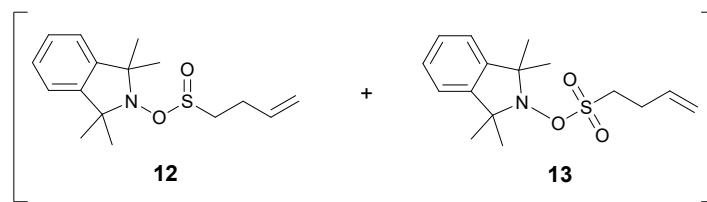
LC-MS of sulfinic acid (14) and sulfonic acid (15)

RT: 4.00 - 12.00 SM: 15B

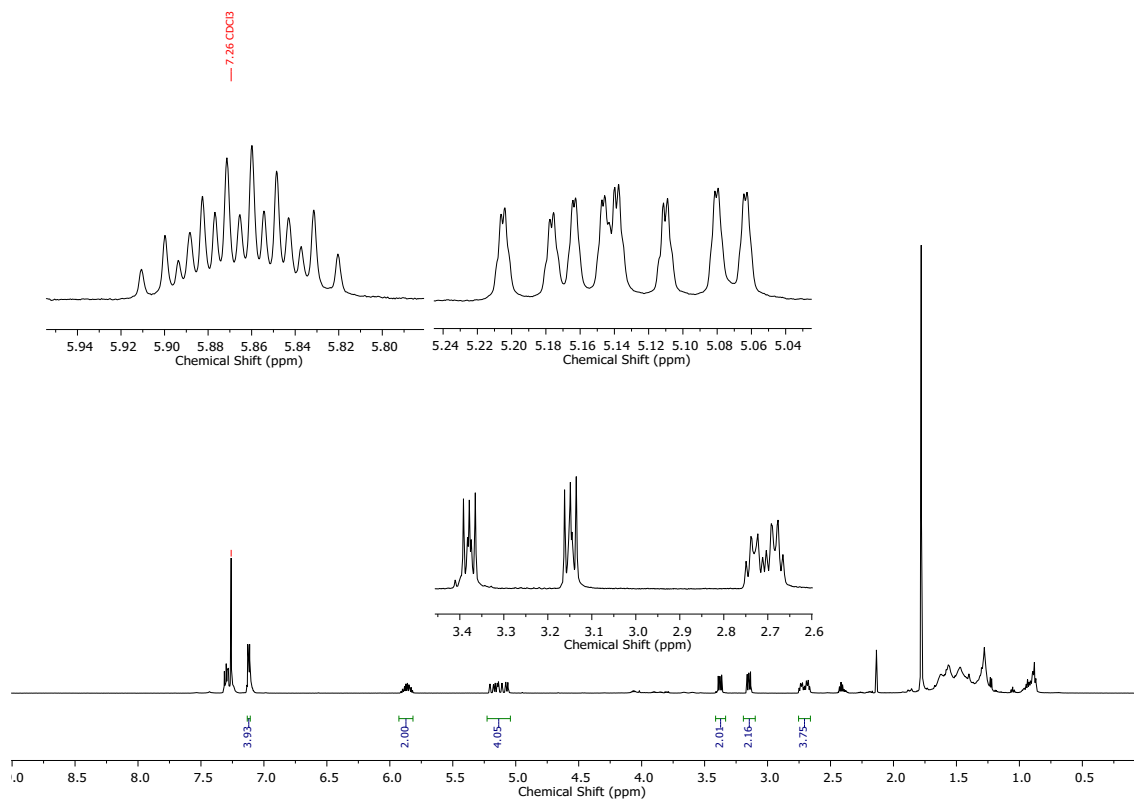


Supplementary Figure 33. LC-MS analysis of crude sample from the Fe-catalysed reaction of H_2O_2 with THTO in the presence of nitroxide 1 after 1.5 h (Table 1, Entry 1). (a.) HPLC chromatogram. (b.) HRMS (ESI) of the HPLC peak at 7.79 min. (c.) HRMS (ESI) of the HPLC peak at 8.11 min.

NMR of isolated sulfinic ester (12) and sulfonic ester (13) mixture

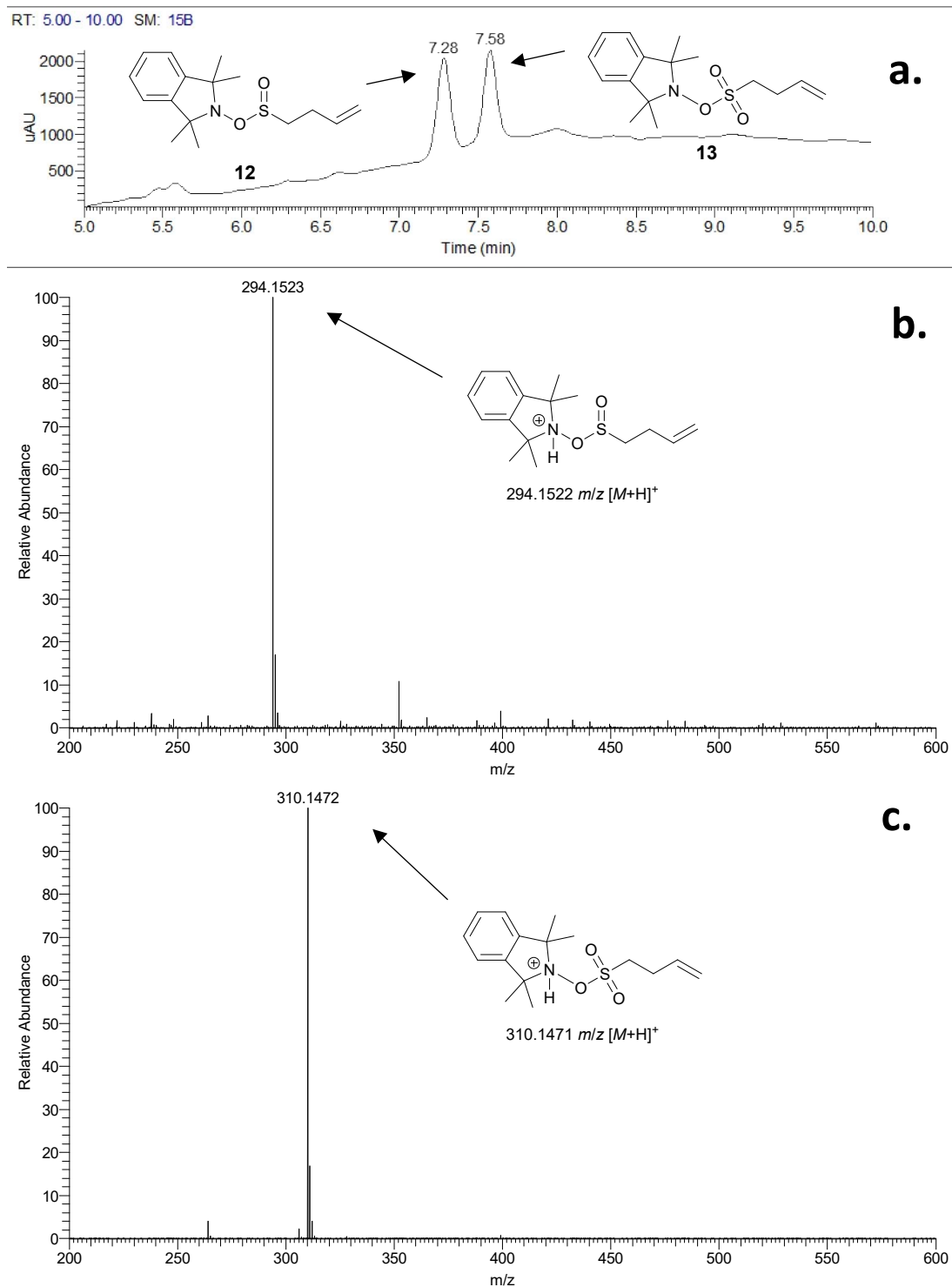


inseparable mix



Supplementary Figure 34. ¹H NMR (600 MHz, CDCl₃) of the (12)-(13) mixture.

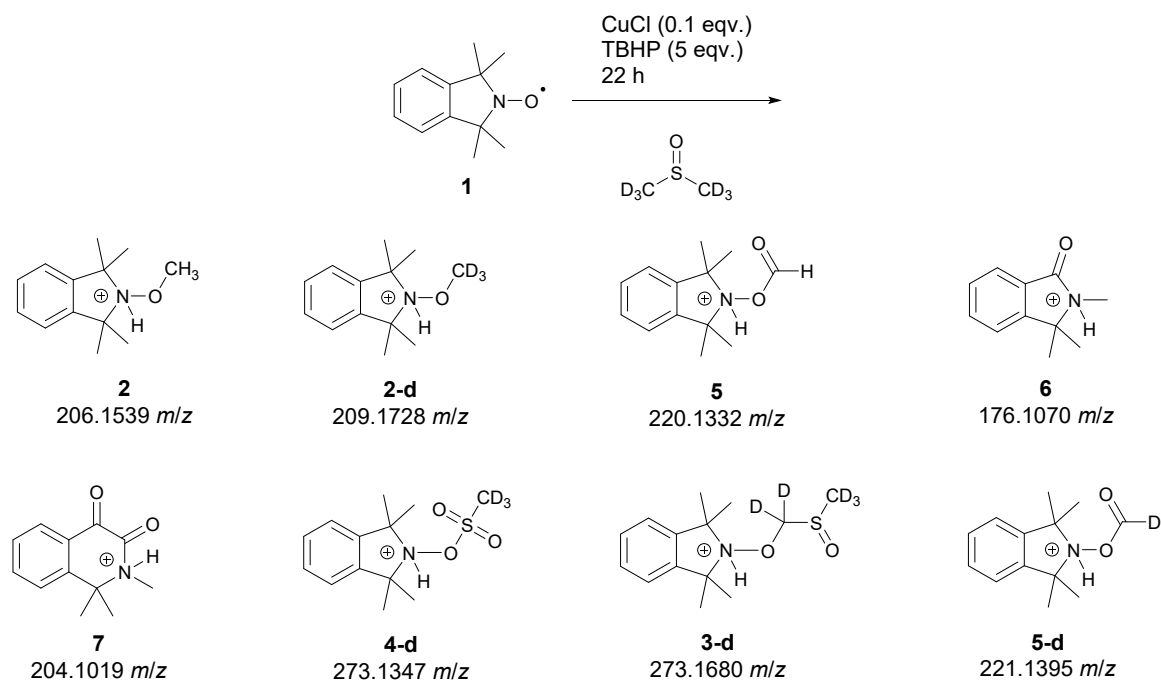
LC-MS of isolated sulfenic ester (12) and sulfonic ester (13) mixture



Supplementary Figure 35. Analytical C18 RP-HPLC-HRMS (ESI) analysis of the (12)-(13) mixture. (a.) HPLC chromatogram. (b.) HRMS (ESI) of the HPLC peak at 7.28 min. (c.) HRMS (ESI) of the HPLC peak at 7.58 min.

D6-DMSO Experiment

Table 3. Products observed by LC-MS from the copper-catalysed reaction of TBHP with d₆-DMSO in the presence of nitroxide **1**.



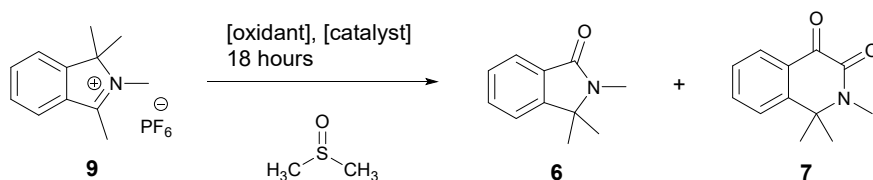
Structure	Molecular Ion	<i>t_R</i> (min)	Calcd. <i>m/z</i>	Observed <i>m/z</i>	Intensity (%) ^[a]
2	C ₁₃ H ₂₀ NO ⁺ [<i>M</i> +H] ⁺	11.13	206.1539	206.1540	1.007
2-d	C ₁₃ H ₁₇ D ₃ NO ⁺ [<i>M</i> +H] ⁺	11.13	209.1728	209.1728	1.182
3-d	C ₁₄ H ₁₇ D ₅ NO ₂ S ⁺ [<i>M</i> +H] ⁺	3.78	273.1680	273.1685	12.94
4-d	C ₁₃ H ₁₇ D ₃ NO ₃ S ⁺ [<i>M</i> +H] ⁺	3.84	273.1347	273.1362	3.678
5	C ₁₃ H ₁₈ NO ₂ ⁺ [<i>M</i> +H] ⁺	5.10	220.1332	220.1336	0.627
5-d	C ₁₃ H ₁₇ DNO ₂ ⁺ [<i>M</i> +H] ⁺	5.10	221.1395	221.1397	0.005
6	C ₁₁ H ₁₄ NO ₂ ⁺ [<i>M</i> +H] ⁺	2.47	176.1075	176.1074	100.0
7	C ₁₂ H ₁₄ NO ₂ ⁺ [<i>M</i> +H] ⁺	2.18	204.1019	204.1024	41.33

[a] Relative to the intensity observed for ion **6** (1.43×10⁸).

Reactions with Iminium Ion (9)

The following reactions were performed on small scale (10 mg of iminium ion **9**) in DMSO (1 mL). All 7 entries were conducted in parallel on the same day and allowed to run overnight for a total of 18 hours. At this time a sample of 100 μ L was taken from each, diluted into LC-MS grade MeOH and examined by LC-MS.

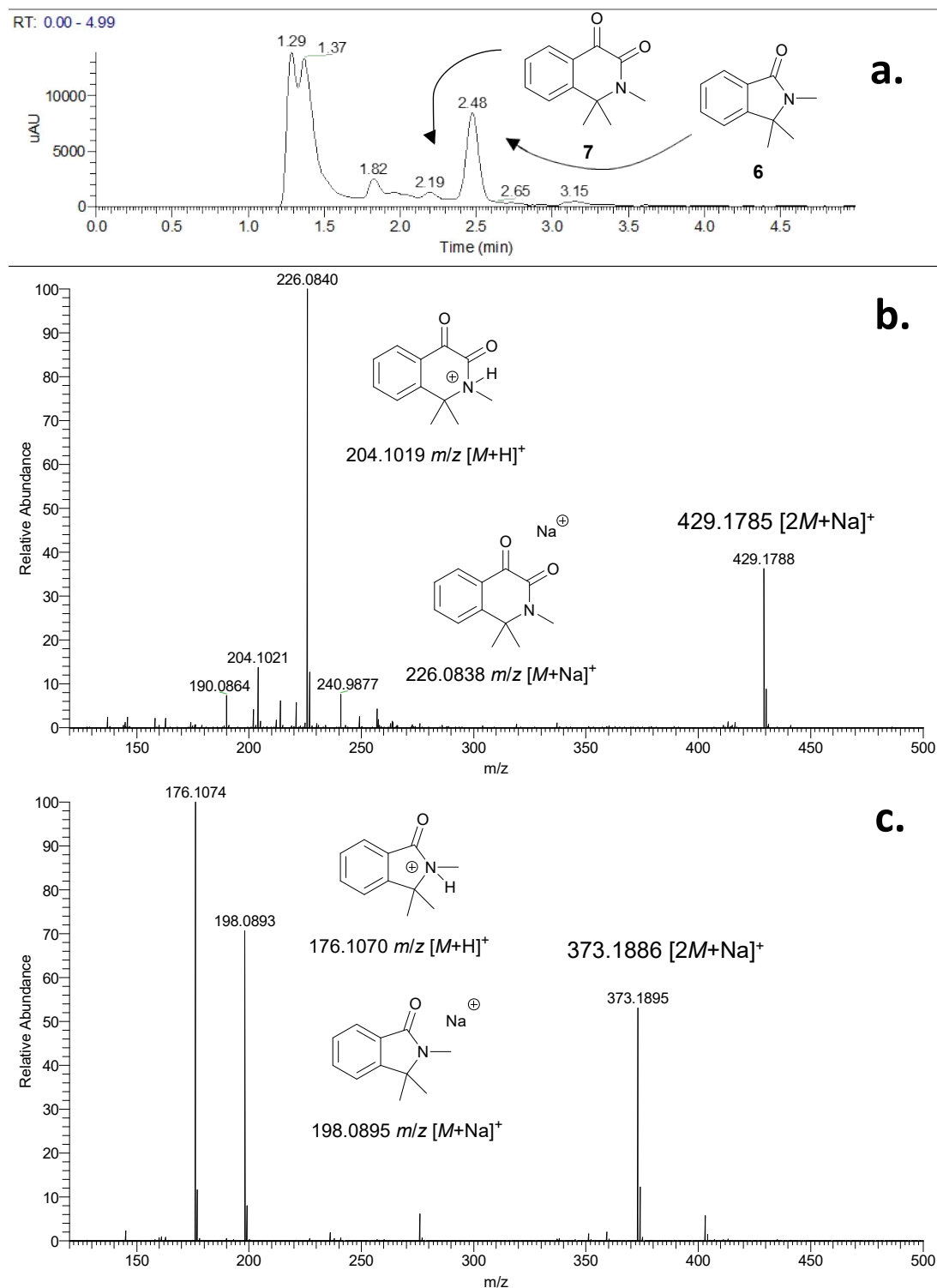
Table 4. Reaction conditions and isolated yields for the Fe(II)/Cu(I)-catalysed reactions of hydrogen peroxide and *tert*-butyl hydroperoxide (TBHP) with DMSO in the presence of nitroxide **1**.



Entry	Oxidant (eqv.) ^[a]	Catalyst (eqv.)	6 t _R (min) ^[b]	7 t _R (min) ^[c]	Found (min) ^[d]
1	H ₂ O ₂ (5.0)	-	-	-	-
2	TBHP (5.0)	-	-	-	-
3	H ₂ O ₂ (5.0)	FeSO ₄ •7H ₂ O (2.5)	-	-	-
4	TBHP (5.0)	FeSO ₄ •7H ₂ O (2.5)	2.47	2.18	-
5	H ₂ O ₂ (5.0)	CuCl (0.1)	-	-	2.18 & 2.47
6	TBHP (5.0)	CuCl (0.1)	-	-	2.19 & 2.48
7	O ₂	-	-	-	-

[a] Hydrogen peroxide (H₂O₂) and TBHP were added to the stirring reaction dropwise whilst oxygen (O₂) was introduced by bubbling compressed air through the solution. [b] Retention time observed from RP-HPLC of (**6**). [c] Retention time observed from RP-HPLC of (**7**). [d] Matching retention times found in the RP-HPLC of the crude reaction sample.

Crude LC-MS of the Cu-catalysed reaction between iminium ion (9) and TBHP (Table 4, Entry 6)



Supplementary Figure 36. LC-MS analysis of the reaction of (9), copper(I) chloride and TBHP in DMSO after 18 hours (Table 4, Entry 6). (a.) HPLC chromatogram. (b.) HRMS (ESI) of the HPLC peak at 2.19 min. (c.) HRMS (ESI) of the HPLC peak at 2.48 min.

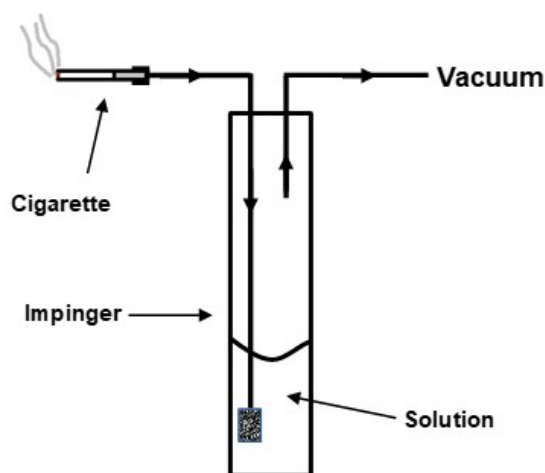
Pollution Derived-PM Experiments

General

Free radicals and reactive oxygen species are recognised components of cigarette smoke¹⁶. The myriad of reactive species, free radicals and oxidised species present are sampled in a number of different ways, including the common approach of transferring them to a solution that is more amenable to subsequent analysis. Typically this is achieved through contact of solvent with bubbles created by an impinger. An impinger is a device used to introduce airborne particles into a liquid medium at a controlled rate. The impinger used in this study was custom made and consisted of a Quickfit Dreschel bottle head, sintered (porosity 1; 100-160 μm pore size) and modified to fit a Quickfit 75 mL test tube (Barloworld Scientific, Staffordshire, UK). The capture efficiency of this impinger was determined by Miljevic *et al.*¹⁴ to be 20-45%, depending on the type and volume of solvent used. The cigarettes used in this study were Kentucky 3R4F reference cigarettes, obtained from University of Kentucky, College of Agriculture Reference Cigarette Program (Lexington, KY).

General Procedure

A solution of DMSO/THTO (10mL) containing nitroxide **1** (25 mM) was placed inside an impinger. The impinger was connected to a vacuum line and cigarette smoke was drawn through the sulfoxide solution until completion at a set flow rate of 1 L min^{-1} regulated by a mass flow controller. This was repeated until a total of ten cigarettes had been used. A 100 μL aliquot of the resulting solution was accurately drawn using a LabCo. single channel pipettor and diluted in LC-MS grade methanol for HPLC-HRMS analysis.



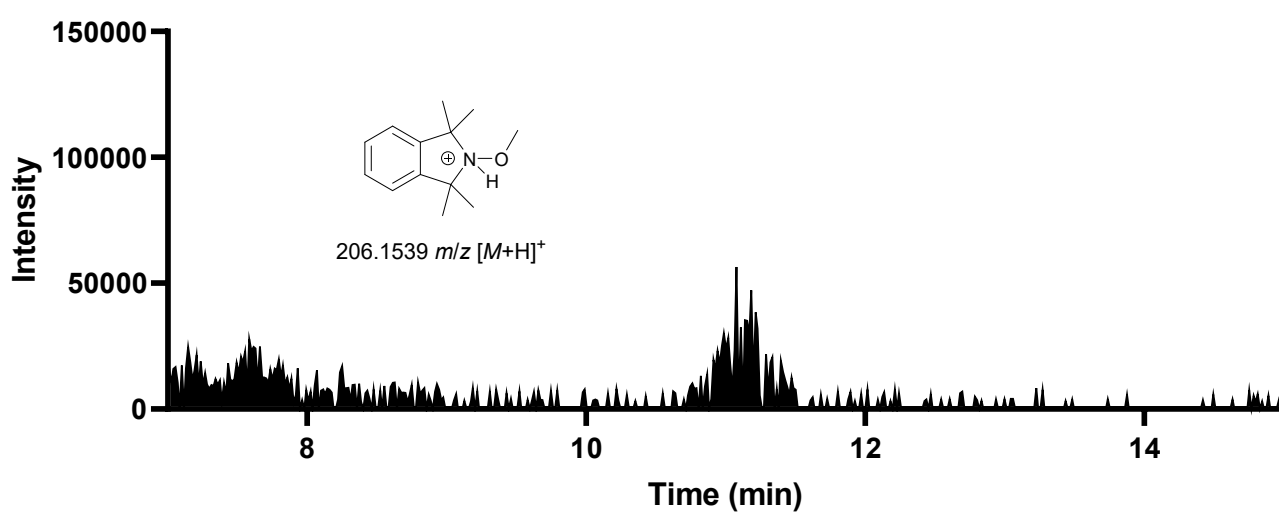
Supplementary Figure 37. Experimental setup for the sampling of mainstream cigarette smoke sampling into a solution. Based on a figure by Miljevic *et al.*¹⁵

LC-MS Data

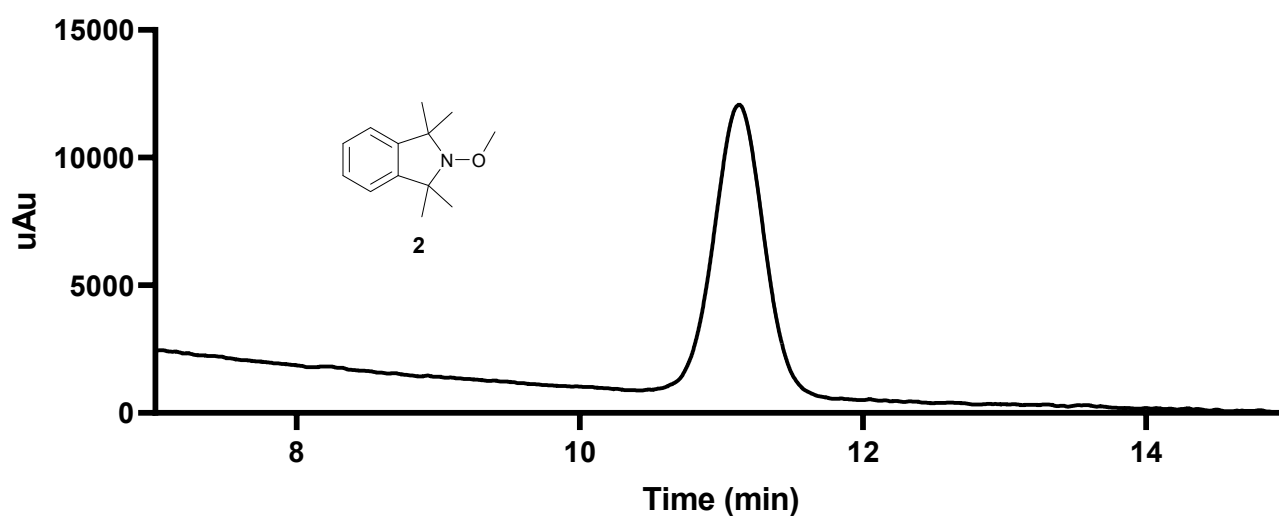
The following chromatograms display the results of conducting a specific mass search (± 5 ppm) using Xcalibur for the particular molecular ion of the previously isolated products within the cigarette smoke exposed sulfoxide solutions. If the search resulted in a mass intensity 'peak' it was compared to the HPLC chromatogram of the authentic product.

General: Analytical C18 RP-HPLC-HRMS (ESI). Solvent A: 0.1% FA in H₂O, Solvent B: MeOH. Isocratic (0.8 mL/min): 20% Solvent A with 80% Solvent B at 40°C detecting at 254 nm. High-resolution mass searches were conducted using the calculated m/z of the subject molecular ion within a mass tolerance of ± 5 ppm.

2-Methoxy-1,1,3,3-tetramethylisoindoline (2)

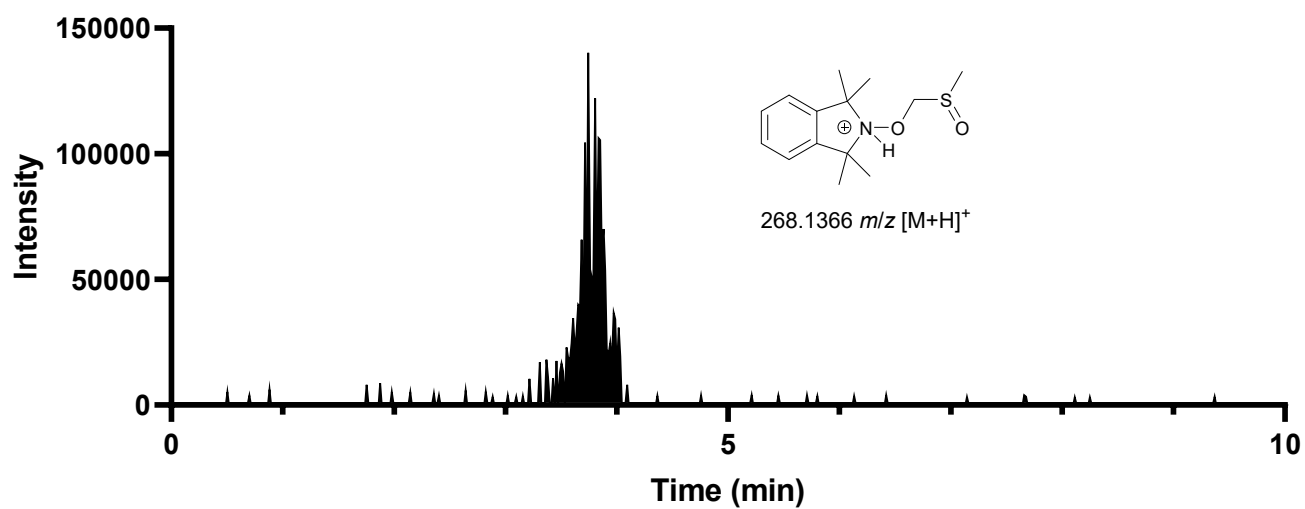


Supplementary Figure 38. Mass search: 206.1539 \pm 0.010.

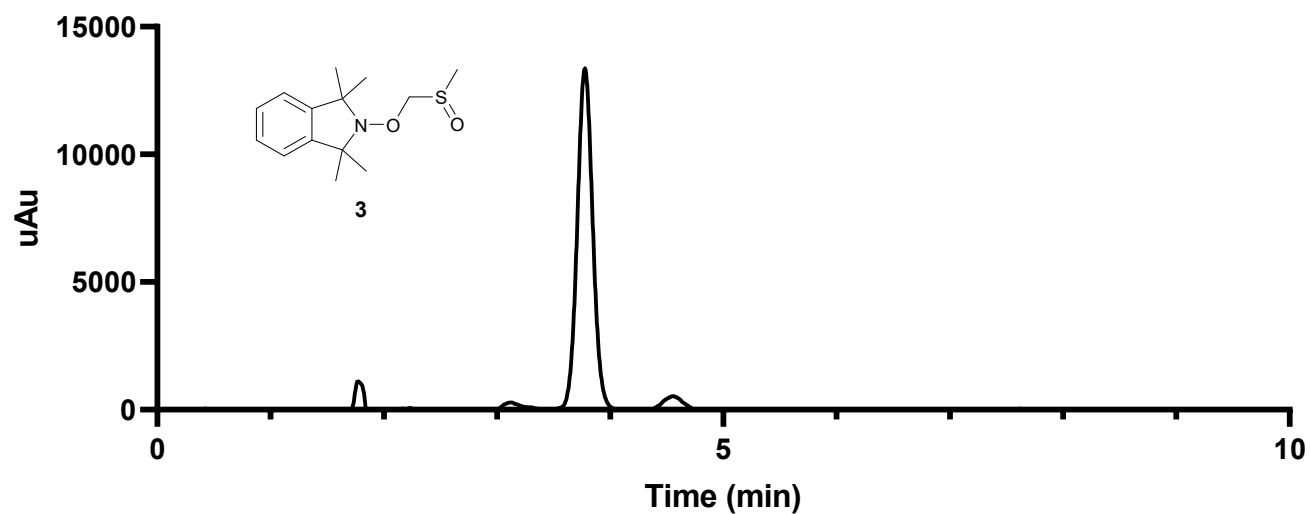


Supplementary Figure 39: HPLC of (2).

1,1,3,3-Tetramethyl-2-((methylsulfinyl)methoxy)isoindoline (3)

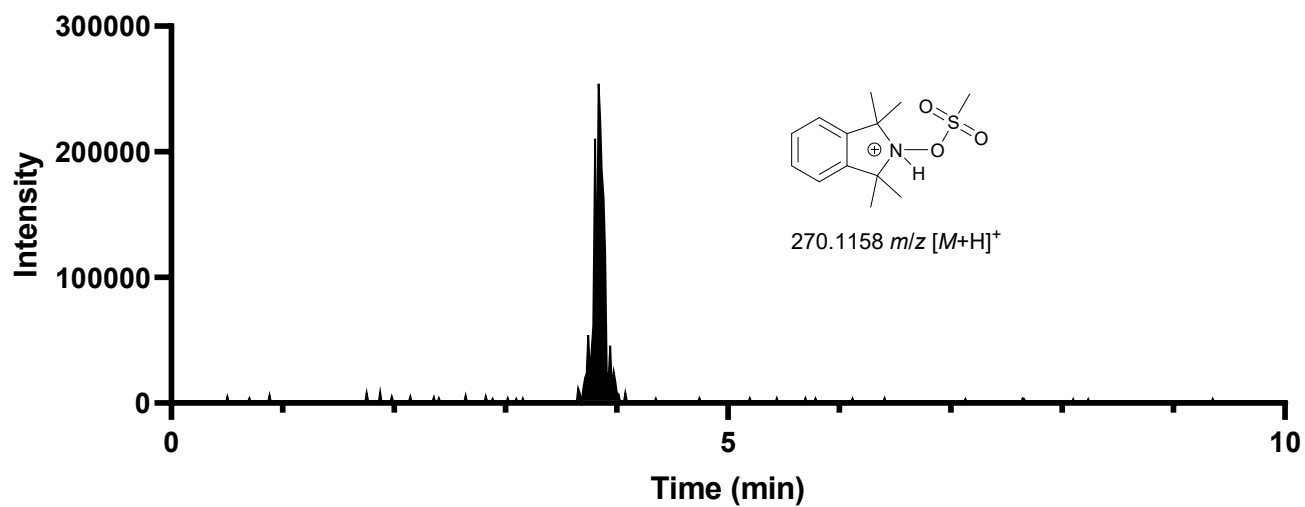


Supplementary Figure 40. Mass search: 268.1366 ± 0.010.

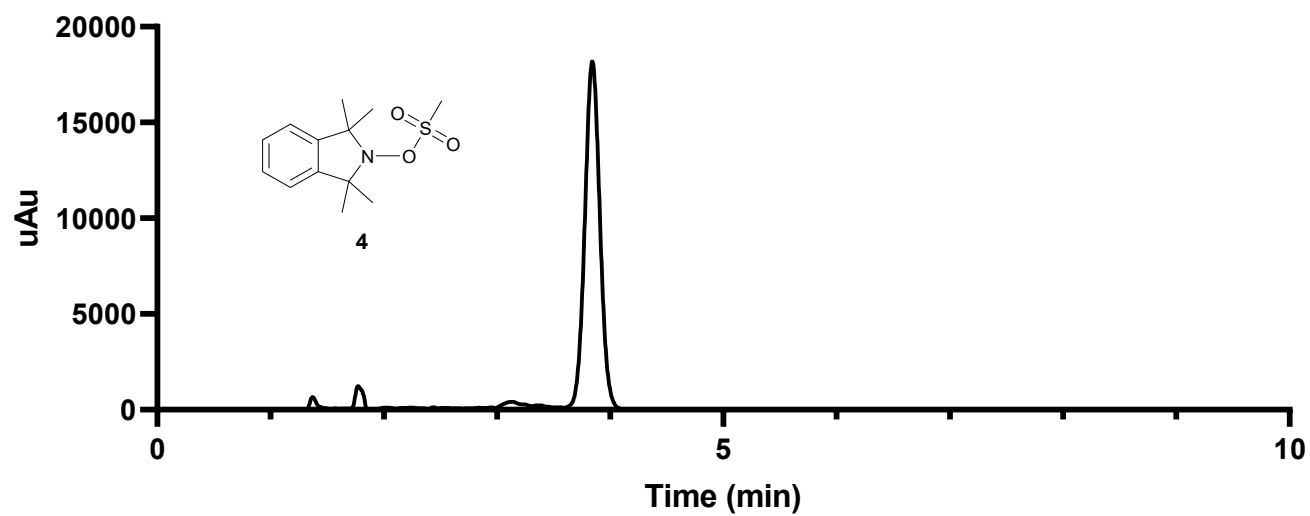


Supplementary Figure 41. HPLC of (3).

1,1,3,3-Tetramethylisoindolin-2-yl methanesulfonate (4)

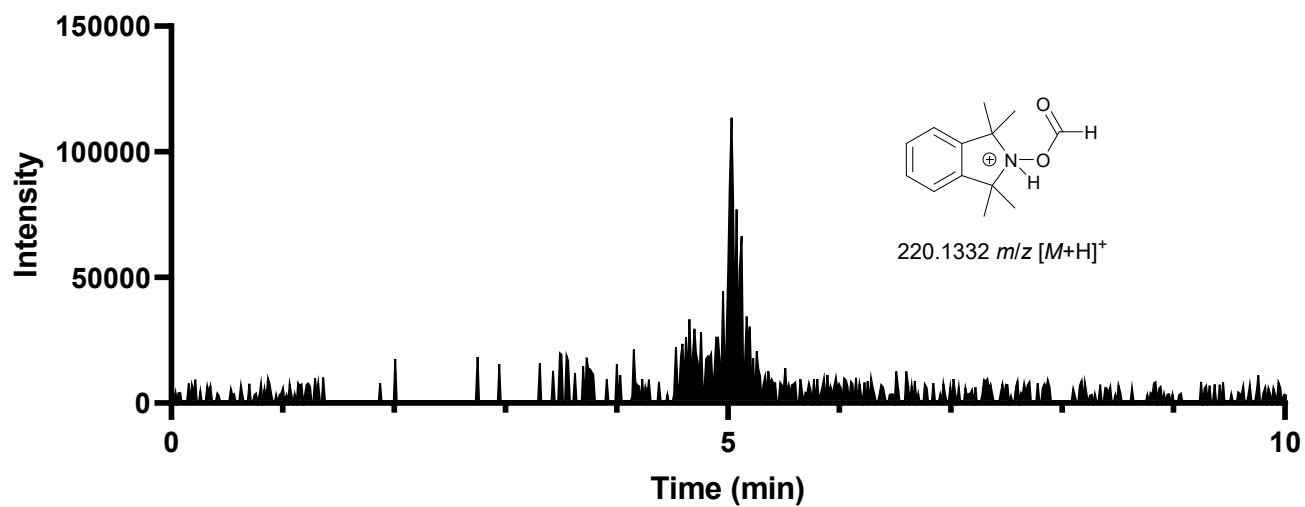


Supplementary Figure 42. Mass search: 268.1366 ± 0.010 .

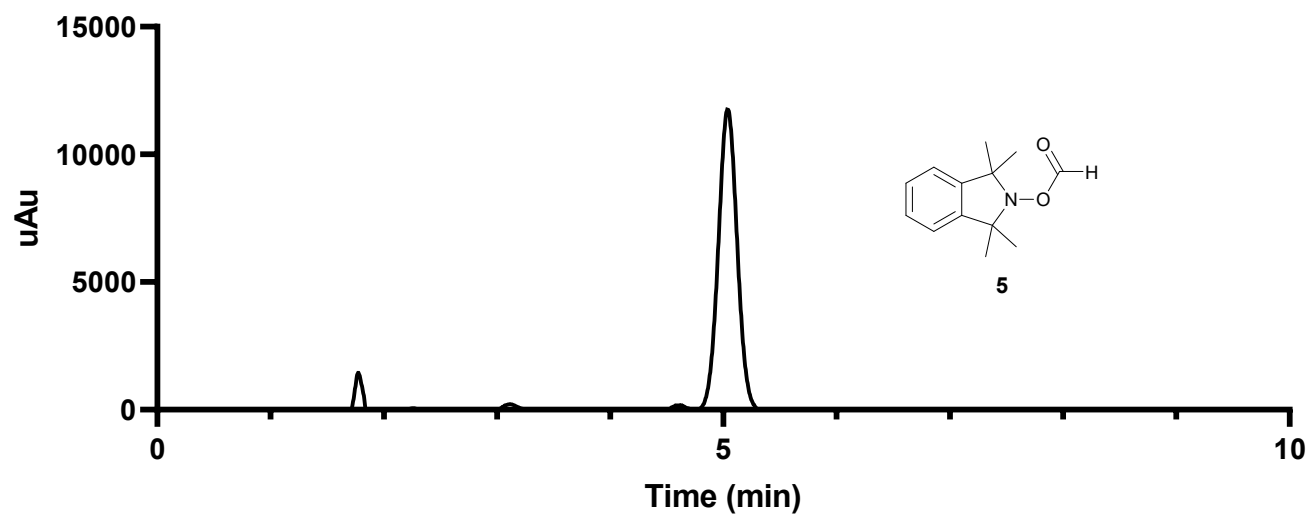


Supplementary Figure 43. HPLC of (4).

1,1,3,3-Tetramethylisoindolin-2-yl formate (5)

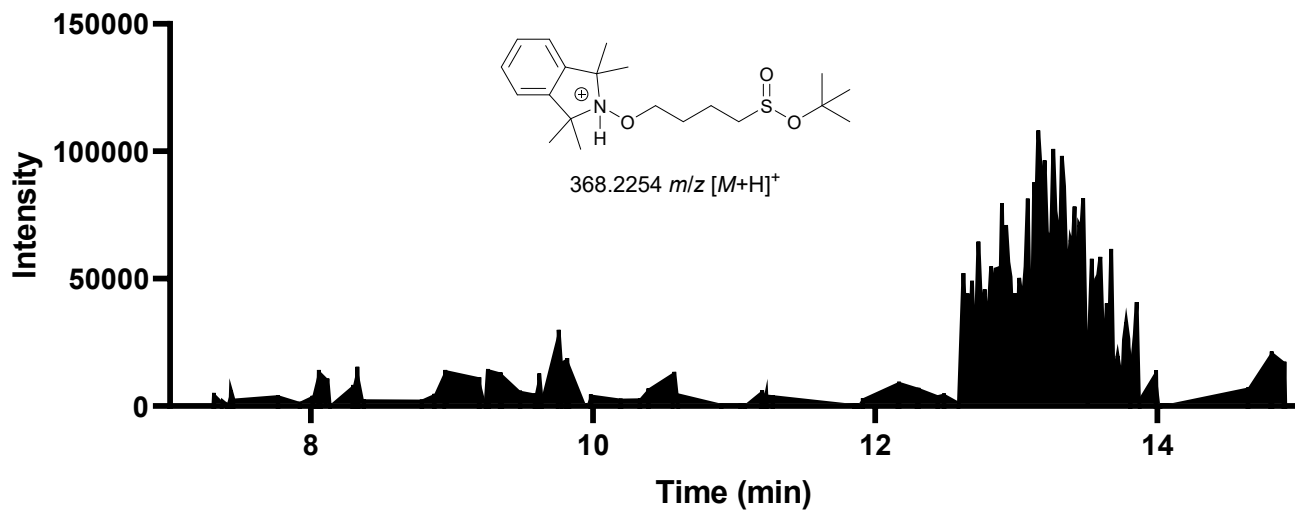


Supplementary Figure 44. Mass search: 220.1332 \pm 0.010.

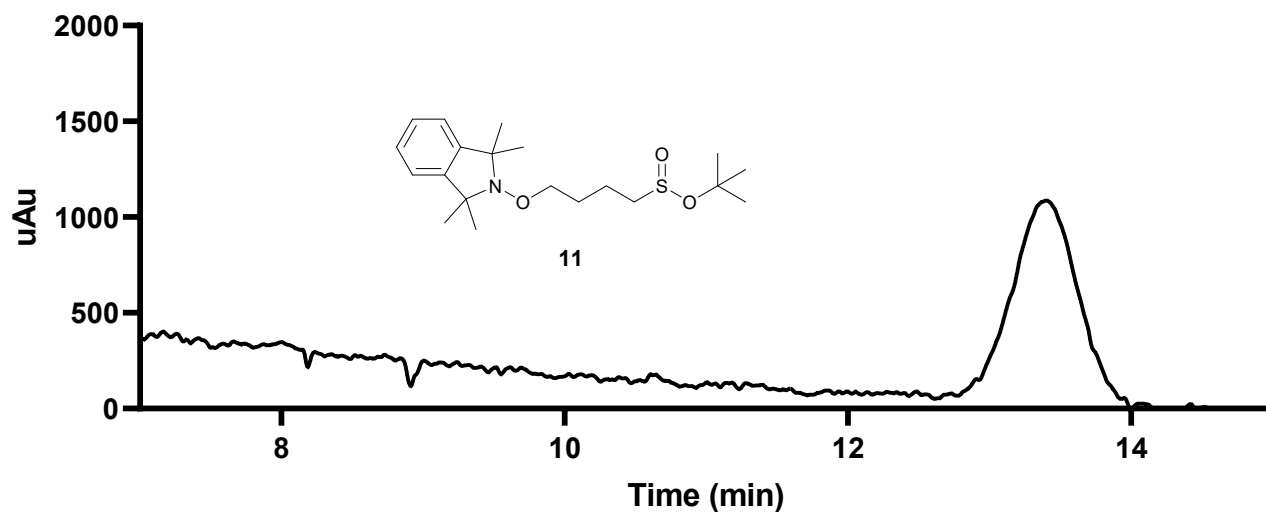


Supplementary Figure 45. HPLC of (5).

Tert-butyl 4-((1,1,3,3-tetramethylisoindolin-2-yl)oxy)butane-1-sulfinate (11)



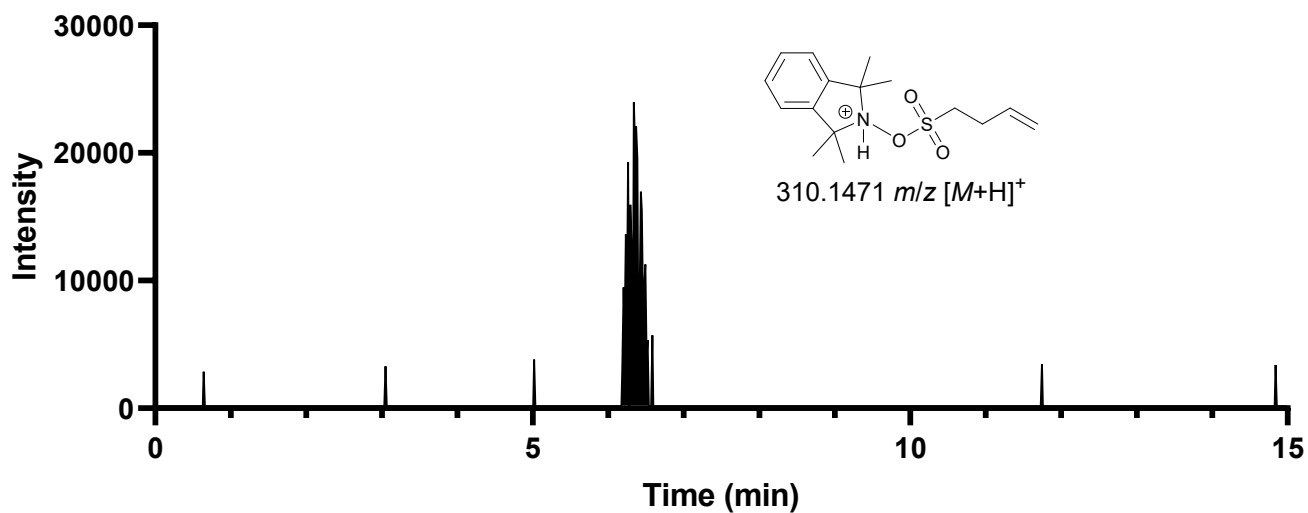
Supplementary Figure 46. Mass search: 368.2254 \pm 0.010.



Supplementary Figure 47. HPLC of (11).

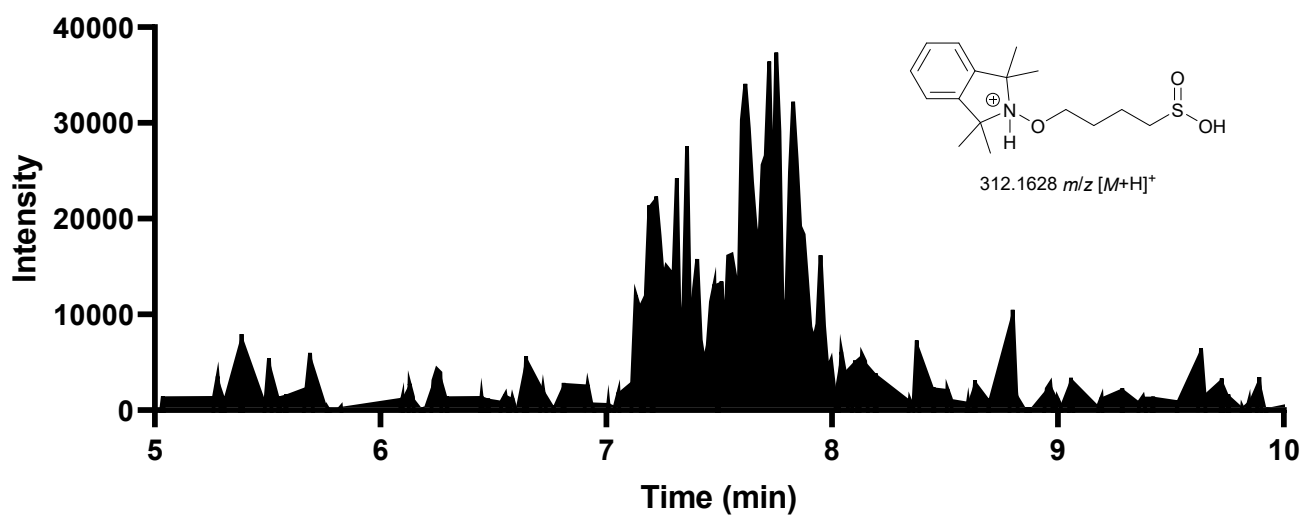
Note: The following mass search chromatograms are for observed products (**12**, **14** and **15**) which were not isolated compounds and therefore do not have an accompanying authentic HPLC trace.

Sulfonic ester (**13**)



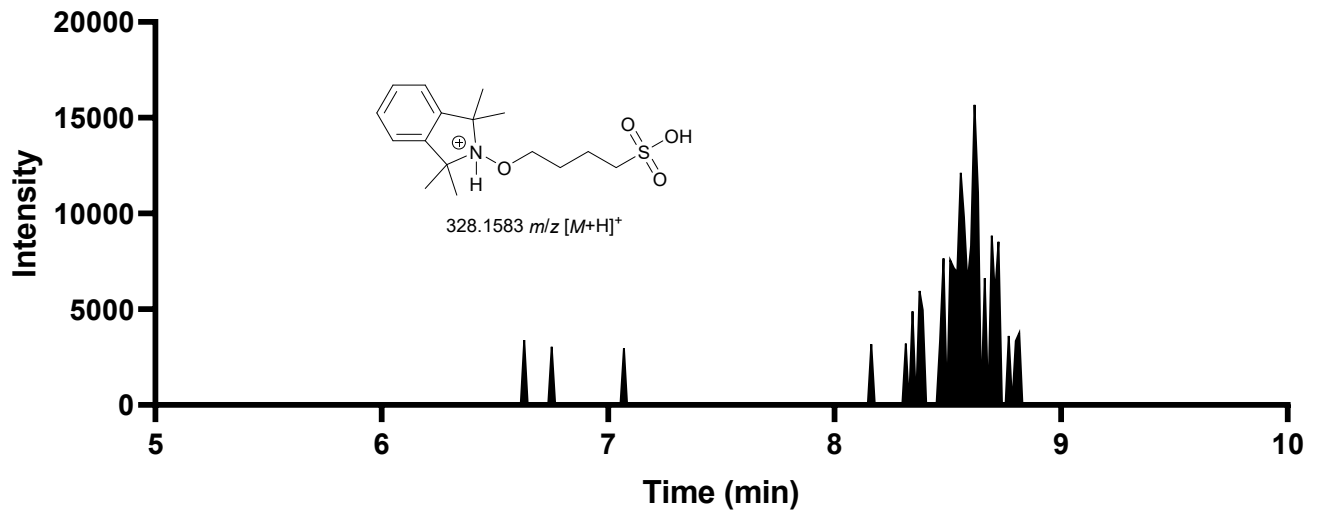
Supplementary Figure 48. Mass search: 310.1471 ± 0.010 .

Sulfinic acid (**14**)



Supplementary Figure 49. Mass search: 312.1628 ± 0.010 .

Sulfonic acid (15)



Supplementary Figure 50. Mass search: 328.1583 ± 0.010 .

References

1. W. L. Armarego, *Purification of laboratory chemicals*, Butterworth-Heinemann, 2017.
2. J. Österlof, C. G. Carlsson, M. Webb and M. Rottenberg, *Acta Chemica Scandinavica*, 1950, **4**, 374-385.
3. K. S. Chan, X. Z. Li and S. Y. Lee, *Organometallics*, 2010, **29**, 2850-2856.
4. P. G. Griffiths, G. Moad and E. Rizzardo, *Aust. J. Chem.*, 1983, **36**.
5. I. Wessely, V. Mugnaini, A. Bihlmeier, G. Jeschke, S. Bräse and M. Tsotsalas, *RSC Adv.*, 2016, **6**, 55715-55719.
6. X. F. Cheng, T. Wang, Y. Li, Y. Wu, J. Sheng, R. Wang, C. Li, K. J. Bian and X. S. Wang, *Org. Lett.*, 2018, **20**, 6530-6533.
7. D. Aragao, J. Aishima, H. Cherukuvada, R. Clarken, M. Clift, N. P. Cowieson, D. J. Ericsson, C. L. Gee, S. Macedo, N. Mudie, S. Panjikar, J. R. Price, A. Riboldi-Tunnicliffe, R. Rostan, R. Williamson and T. T. Caradoc-Davies, *J. Synchr. Rad.*, 2018, **25**, 885-891.
8. W. Kabsch, *Acta Cryst. A*, 2010, **66**, 125-132.
9. G. M. Sheldrick, *Acta Cryst. A*, 2015, **71**, 3-8.
10. G. Sheldrick, *Acta Crystallographica Section C*, 2015, **71**, 3-8.
11. O. V. Dolomanov, L. J. Bourhis, R. J. Gildea, J. A. K. Howard and H. Puschmann, *J. Appl. Cryst.*, 2009, **42**, 339-341.
12. N. P. Cowieson, D. Aragao, M. Clift, D. J. Ericsson, C. Gee, S. J. Harrop, N. Mudie, S. Panjikar, J. R. Price, A. Riboldi-Tunnicliffe, R. Williamson and T. Caradoc-Davies, *J. Synchr. Rad.*, 2015, **22**, 187-190.
13. *Journal*, 2019.
14. B. Miljevic, R. L. Modini, S. E. Bottle and Z. D. Ristovski, *Atmos. Environ.*, 2009, **43**, 1372-1376.
15. B. Miljevic, K. E. Fairfull-Smith, S. E. Bottle and Z. D. Ristovski, *Atmos. Environ.*, 2010, **44**, 2224-2230.
16. W. A. Pryor and K. Stone, *Ann. NY Acad. Sci.*, 1993, **686**, 12-27.